Brain Imaging and Behavior (2011) 5:329–348
DOI 10.1007/s11682-011-9135-2

ORIGINAL RESEARCH

Correlations between EEG and clinical outcome in chronic neuropathic pain: surgical effects and treatment resistance

Lars Michels · Morteza Moazami-Goudarzi · Daniel Jeanmonod

Published online: 27 September 2011

Abstract Chronic neuropathic pain may require a neurosurgical treatment, but for reasons that have not been fully explored yet, a significant number of patients do not benefit from the intervention. We compared the resting EEG of 15 healthy controls to the EEG of 23 chronic neuropathic pain patients before and 12 months after treatment by the central lateral thalamotomy (CLT). A patient subgroup had a high (n=14, pain relief (PR)≥50%) and another subgroup a low (n=9, PR<50%) postoperative PR. EEG spectral power and source localization of the high PR patients were normalized postoperatively. In contrast, low PR patients showed postoperative maintenance of insular, cingulate and prefrontal overactivities, and their frustration values were positively correlated with cingulate and prefrontal activity. These findings demonstrate a normalizing effect of CLT on cortical activity and suggest that treatment resistance is associated with a frustration-based dynamics.

Keywords Neuropathic pain · EEG · LORETA · Central lateral thalamotomy · Frustration · Treatment resistance

Abbreviations

ACC	anterior cingulate cortex
CLp	central lateral thalamic nucleus, posterior part
CLT	central lateral thalamotomy
EEG	electroencephalography
FDR	false discovery rate
FFT	fast Fourier transform
HC	healthy controls
HPR	high pain relief
IC	insular cortex
aIC	anterior IC
pIC	posterior IC
ICA	independent component analysis
ITC	inferotemporal cortex
LPR	low pain relief
LORETA	low resolution brain electromagnetic tomography
LTS	low threshold calcium spikes
MEG	magnetoencephalography
MCC	midcingulate cortex
mTC	medial temporal cortex
NP	neuropathic pain
OFC	orbitofrontal cortex
OC	occipital cortex
PCC	posterior cingulate cortex
PFC	prefrontal cortex
mPFC	medial PFC
lPFC	lateral PFC
ROI	region of interest
TCD	thalamocortical dysrhythmia
TPC	temporoparietal cortex
VAS	visual analogue scale

Lars Michels and Morteza Moazami-Goudarzi contributed equally to this work.

L. Michels (✉) · M. Moazami-Goudarzi · D. Jeanmonod
Laboratory for Functional Neurosurgery,
University Hospital Zurich,
CH-8091 Zurich, Switzerland
e-mail: lars.michels@uzh.ch

M. Moazami-Goudarzi
Institute of Neuroinformatics, ETHZ/UNIZH,
Winterthurerstrasse 190,
8057 Zurich, Switzerland

D. Jeanmonod
Center for Integrative Human Physiology, University of Zürich,
8057 Zurich, Switzerland

Introduction

Pain is defined as an unpleasant sensory and emotional experience that arises from actual or potential tissue damage. The central processing of pain is known to rely on a neural network involving several cortical and thalamic brain areas (Melzack and Casey 1968). In healthy controls, studies identified via brain imaging methods such as functional magnetic resonance imaging (fMRI) the neuronal correlates to an applied exogenous nociceptive stimulus (Apkarian et al. 2005; Chen et al. 2008; Dube et al. 2009; Moisset and Bouhassira 2007; Peyron, Laurent, and Garcia-Larrea 2000a; Tracey 2005, 2007). This so-called "pain matrix" includes the thalamus, anterior and posterior insular cortex (aIC and pIC), lateral and medial prefrontal cortex, (lPFC and mPFC), anterior-, mid- and posterior cingulate cortex (ACC, MCC, PCC), primary and secondary somatosensory cortex (S1 and S2), orbitofrontal cortex (OFC), basal ganglia, premotor cortex, midbrain, cerebellum, and posterior parietal cortex (PPC). The results indicate that pain, as large portions of the paralimbic and associative cortical areas are concerned, is a complex phenomenon which requires the tight integration of sensory but also emotional (Talbot et al. 1991), motivational, and other cognitive dimensions (Treede et al. 1999). However, it has to be noted that some of these brain areas (e.g., PPC) are not only pain-related regions but are also linked to general attention (Iannetti et al. 2008; Legrain et al. 2011) or salience function (Downar et al. 2002, 2003).

Another "pain matrix" to be defined is the one reflecting chronic neuropathic pain (NP, synonym: neurogenic) states. NP is caused by a damage of the peripheral or central pain pathways and is characterized by pain perception in the absence of peripheral nociceptive stimulation. NP represents a most significant clinical problem and may resist all therapies. Many studies using imaging and electrophysiological techniques have examined the cortical and subcortical representation of pain (Bingel et al. 2002; Bornhovd et al. 2002; Buchel et al. 2002; Garcia-Larrea et al. 2003; Petrovic et al. 2004; Ploner et al. 2002; Shibasaki 2004; Treede et al. 2003) and NP (Hsieh et al. 1995; Llinás et al. 1999; Shulman et al. 2005; Walton et al. 2010; Willoch et al. 2000; Wydenkeller et al. 2009). Electroencephalography (EEG) and magnetoencephalography (MEG) studies have shown that NP is associated with increased low (theta: 4–7 Hz and alpha: 8–13 Hz) and high (beta: 13–30 Hz) frequency band power (Boord et al. 2008; Llinás et al. 1999; Sarnthein et al. 2006; Schulman et al. 2005; Stern et al. 2006). These spectral power increases occurred in all cortical partners of the above-mentioned nociceptive pain matrix, so that a NP matrix globally identical with it may be proposed (Stern et al. 2006). However, only few studies have examined the brain responses after neurosurgical intervention in NP patients (Sarnthein et al. 2006; Stern et al. 2006). So far there is no study available that compared pre- and postsurgical interactions between spectral EEG power, source localization, and clinically relevant parameters such as pain relief (PR). Examining the interactions between these variables might help to understand the link between pain, suffering, and relief (Lee and Tracey 2010). Further, the question about how brain activity differs in patients with a high and a low PR has not been addressed yet. Are EEG overactivities still to be found in patients with a low PR? If present, such overactivities are expected to be found spread in the large cognitive-emotional (paralimbic-associative) cortical matrix, which contains, with the exception of S1 and S2, the whole NP matrix. The surgical tool used in this study is the central lateral thalamotomy (CLT), which is a reactualized form of medial thalamotomy developed on the basis of pathophysiological data collected with microelectrode single unit recordings during stereotactic operations in the medial thalamus (Jeanmonod et al. 1996; Jeanmonod and Morel 2009). First evidence for a normalization of EEG overactivities after CLT has been published by Stern et al. (2006) and Sarnthein et al. (2006).

The aim of this study was to examine chronic NP patients with different levels of postsurgical PR. Our primary hypothesis was that patients with a low postsurgical PR would demonstrate the maintenance of EEG overactivities, whereas the EEG of patients with a high PR would show reduced overactivities or even a normalization. From the analysis of correlations between EEG and clinical parameters, we hoped in addition to identify associations between negative emotional factors (i.e., frustration, anxiety, and depression) and cortical overactivities.

Material and methods

Patients

We recorded the EEG before (baseline) and 12 months after the CLT from 23 NP patients (mean age at CLT: 58 years± 7 years, 13 males) who fulfilled the criteria for a surgical therapy, namely clear NP diagnosis, chronicity (chronic pain state >1 year), drug therapy-resistance (at least antiepileptic drugs, benzodiazepines, and antidepressants), and a strongly diminished quality of life. The EEG data of 5 patients have been used in a previous study of our group (Stern et al. 2006). The study falls under the ethical approval of the 'Kantonale Ethikkommission Zürich' (reference number: KEK-StV-Nr.05/03*). All patients and control subjects were fully informed about the aim and the scope of the study and gave written informed consent. Biographic data, such as description of pain causes, side, localization and duration, is reported in Table 1. Clinical

Table 1 Illustration of the biographic data. SD indicates the standard deviation

High pain relief (HPR) group						
pat.	gender	age (years)	pain cause	pain location	pain side	pain duration (years)
1	female	69	peripheral	trigeminus	right	14
2	male	61	central	leg	bilateral	2
3	female	54	peripheral	leg	left	8.5
4	female	58	central	trigeminus	right	8
5	female	54	peripheral	arm	right	16
6	male	66	central	trigeminus	right	6
7	female	51	peripheral	trigeminus	right	3
8	male	38	peripheral	trigeminus	right	13
9	male	64	peripheral	leg	left	13
10	male	50	peripheral	trigeminus	left	4.5
11	male	59	peripheral	trigeminus	left	5
12	female	52	peripheral	trigeminus	left	1.5
13	male	68	peripheral	trigeminus	right	1
14	female	58	peripheral	leg	left	7
Mean (SD)		57 (8.3)				7.3 (5)
Low pain relief (LPR) group						
1	male	71	central	hemibody	right	5
2	female	50	peripheral	trigeminus	right	7
3	male	59	peripheral	trigeminus	left	2
4	male	57	peripheral	arm	right	6.5
5	male	52	peripheral	trigeminus	right	4
6	female	60	peripheral	trigeminus	right	5
7	female	58	peripheral	trigeminus	right	1.5
8	male	62	peripheral	leg	right	3
9	male	56	peripheral	arm	right	7
Mean (SD)		58 (6.1)				4.6 (2.1)
HPR - LPR (p-values)		0.749				0.131

data of the patients (Tables 1 and 2) were collected before (baseline) and 12 months after the CLT by an experienced neurosurgeon and psychiatrist. The clinical data comprise of a five-scale rating for decrease of quality of life (QOL), depression, anxiety and frustration, mean pain intensity (not the affect of pain) estimation on a Visual Analogue Scale (VAS), medications, side of surgery and PR (Table 2). The VAS 100 mm line was presented to the patients who had to move the cursor to the positions (0-100/100) corresponding to the slightest and the worst pain intensities experienced, without seeing the millimeter values. The VAS has been used in many studies for pain quantification (Chanda et al. 2011; Poliakov and Toth 2011) In Table 2, we entered the mean VAS values, (i.e. the mean of the maximum and the minimum positions). The pain evolution assessment with VAS measurements was complemented by the use of a patient rating of the experienced global PR (in%), where 0% represents an unchanged pain state after the operation and 100% a complete PR. To assess the level of depression, anxiety and frustration as well as the decrease of quality of life, we used a scale ranging from 0 to 4 which was presented verbally to the patients. For depression, anxiety and frustration, zero indicates the absence, 1 a slight, 2 a moderate, 3 a strong and 4 a massive intensity level. For decrease of quality of life, 0 is for an absent, 1 a slight, 2 a moderate, 3 a strong and 4 a massive decrease. In Table 2, the 0.5 values are due to the situations where patients could not decide between two consecutive positions (e.g. 2.5 for a scoring between 2 and 3). We used the decrease of quality of life to get a value moving in the same direction as the 3 emotions, thus simplifying the comparisons and the analyses. It also made the task easier for the patients: they could concentrate on their amount of suffering and not on what would be a "normal quality of life".

To assess between-group differences on the behavioral level, two-sample (two-tailed) t-tests are used for patients' age, pain duration, decrease of quality of life, pain intensity and PR. As the data from psychological scores are ordinal in nature, and therefore the assumptions of the *t*-test are violated, non-parametric tests

Table 2 Illustration of the pre- and post-surgery clinical data for patients with a high pain relief (HPR) and for patients with a low pain relief (LPR)

High pain relief (HPR) group																				
pat.	Pre-surgery									Post-surgery (12 month)										
	Decrease of QOL	Mean pain intensity (VAS)	Psychological scores			Medication				Decrease of QOL	Mean pain intensity (VAS)	Psychological scores			Pain relief (%)	CLT side	Medication			
			D	A	F	AE	AD	O	B/O			D	A	F			AE	AD	O	B/O
1	3	70	3	0	2	x	x	x	x	0	65	3	1	3	50	bilat.	x	x		x
2	3.5	70	1	1	1	x	x			0	0	0	0	0	100	bilat.			none	
3	3.5	60	0	0	2	x		x		1.5	40	0	0	0	75	right			none	
4	3.5	100	0	0	3	x				0	2	0.5	0.5	0.5	98	bilat.	x	x		x
5	3	70	0	0	3	none				2.5	55	1	0	2	50	bilat.				x
6	4	60	0	0	2	x		x		0	0	0	0	0	100	bilat.			none	
7	3.5	75	2.5	0	3	x	x	x	x	0	55	0	0	0	75	left			x	x
8	3	50	2	2	4	x				0	2	0	0	0	95	bilat.			none	
9	4	60	0	0	0	x	x	x		1	40	0	0	0	80	bilat.			none	
10	4	48	3	1	1	x	x	x	x	1.5	40	1	1	1	50	bilat.	x	x		x
11	1	35	0	0	1	x				0	0	0	0	0	100	right			none	
12	4	80	1	2	3	x			x	0.5	45	0.5	0	1	70	bilat.			none	
13	3.5	70	1	0	0	none				0	0	0	0	0	100	bilat.			none	
14	4	43	2	3	3	x	x	x	x	0.5	50	0	0.5	0.5	93	bilat.		x		x
Mean (SD)	3.4 (0.8)	63.3 (16.6)	1.1 (1.2)	0.6 (1)	2 (1.2)					0.5 (0.8)	28.1 (25.6)	0.4 (0.8)	0.2 (0.4)	0.6 (0.9)	81.1 (19.9)					
Low pain relief (LPR) group																				
1	3.5	72	2	0	3.5		x	x	x	2	71	2	0	2	40	bilat.		x		x
2	1	54	3.5	3.5	3.5	x	x	x	x	1	25	2	1.5	2	30	right		x		x
3	3	67	2	2	2.5	x			x	2.5	63	2	2	4	35	right		x		x
4	2.5	65	2.5	2	2		x	x	x	2.5	65	2	2	2	0	bilat.		x		x
5	3	50	0	0	2	x		x	x	3	80	0	0	0	−10	left	x			x
6	4	88	3	3	4	x	x	x	x	3	76	3	2	4	−50	bilat.		x		x
7	2	69	0	0	3				x	2	50	0	0	2	10	left				x
8	3.5	65	1	2	3	x		x	x	3.5	50	2	2	2	−5	bilat.			none	
9	3	55	2	0	1.5	x	x			2.5	50	1.5	0	1.5	0	bilat.			none	
Mean (SD)	2.8 (0.9)	65 (11.4)	1.8 (1.2)	1.4 (1.4)	2.8 (0.8)					2.4 (0.7)	58.9 (17)	1.6 (1)	1.1 (1)	2.2 (1.2)	5.6 (27.8)					
HPR - LPR (p-values)	0.131	0.833	0.217	0.195	0.131					9.3E-06	0.005	0.012	0.052	0.004						

Abbreviations: *QOL* quality of life, *D* depression; *A* anxiety, *F* frustration. The values for the psychological scores range between 0 (absence of symptomatology) and 4 (massive symptomatology). *VAS* visual analogue scale in mm as a marker for pain intensity (100 mm = max. pain, 0 mm = no pain). VAS is reported for the mean pain (i.e., the mean between minimally and maximally indicated pain) intensity before the EEG recording session; *AE* antiepileptic drugs; *AD* antidepressants; *O* opioids; *B/O* benzodiazepines/others. The bottom line displays statistical results, i.e. p-values of two-tailed two-sample t-tests (QOL, mean pain intensity) or p-values of two-tailed two-sample non-parametric Mann–Whitney U-tests (D, A, and F) for the comparison HPR versus LPR group. For PR, no statistical comparison was performed as this was the grouping variable

(Mann–Whitney U-test, two-tailed) are used to test for between-group differences.

Healthy controls

The healthy control (HC) group consisted of 15 individuals (mean age 62 years±6 years, 8 males). The HC and HPR/LPR groups did not statistically differ in age (both $p>0.1$, unpaired t-test) or gender ($p>0.1$, rank sum test). All HC subjects filled a detailed health questionnaire that checks for a non-morbid state, including questions on psychiatric disorders ('Zürcher Gesundheits-Fragebogen', S. Kuny and H.H. Stassen, 2004) such as depression and anxiety. None of the individuals showed a sign of depression or anxiety. In addition, none of them had any current or previous history of relevant physical, neurological or psychiatric illness, and they were not currently taking drugs or medication known to affect EEG.

Surgery

Neurosurgical therapy for the patients consisted of the central lateral thalamotomy (CLT), corresponding to a therapeutic lesion in the posterior part of the central lateral thalamic nucleus, called CLp (Jeanmonod et al. 2001a; b; 2009; Morel et al. 1997). The CLT stereotactic intervention took place under local anaesthesia. A stereotactic frame (Cosman Robert Wells, Radionics, Burlington Massachusetts) compatible with magnetic resonance (MR) was used. The electrode reached the computer-calculated target in the base of CLp through a prefrontal approach, under impedance monitoring. The coordinates of the CLT target are: (1) dorso-ventral: the intercommissural plane, (2) antero-posterior: 2 mm posterior to the pc, and (3) medio-lateral: 6 mm lateral to the thalamo-ventricular border. Single unit recordings were obtained using tungsten microelectrodes, with a protocol including tests of motor voluntary function, as well as tactile, nociceptive and proprioceptive stimuli. The microelectrode recordings are useful to first localize the ventral border of CLp, and second to demonstrate the lack of responses of most units and the presence of low-threshold calcium spike (LTS) bursts. At the end of the recording session, a macroelectrode replaced the microelectrode in the common guide tube, and a macrostimulation session was performed analysing somatosensory, motor and cognitive/emotional responses. A radiofrequency thermolesion (4 mm diameter over 10–12 mm length) was placed. MR imaging of the CLT lesion was performed 2 days after the surgery on T1-weighted images. A unilateral lesion of one patient is shown in Fig. 1. Often, the CLT must be performed bilaterally (Table 2). The anatomical evidence for this bilaterality is the bilateral spinothalamic projections, particularly significant for axial, face and low extremity inputs. The EEG evidence is presented in Stern et al. (2006) and Sarnthein et al. (2006) showing that the EEG overactivities are indeed localized bilaterally. The clinical evidence was already present in the literature and has been reviewed and confirmed (Jeanmonod and Morel 2009). Few patients had only a unilateral CLT, either because the obtained PR was sufficient, or because of the presence of dominant counterproductive postoperative

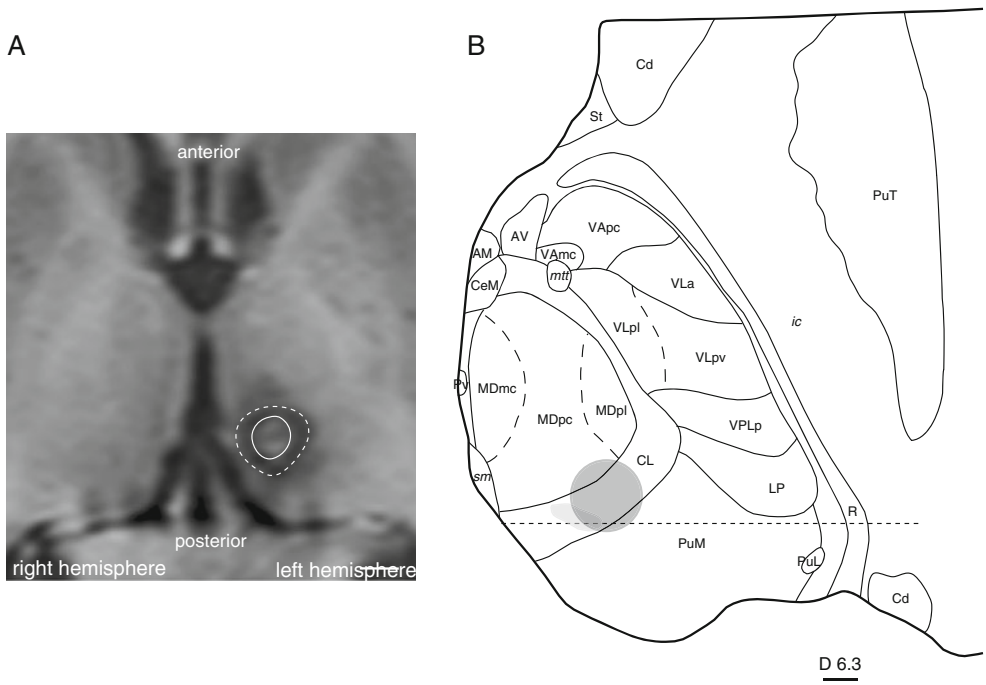

Fig. 1 Illustration of postoperative 3-D MRI (**a**) and horizontal atlas projections **b** of a unilateral CLT lesion in a single patient. The outline of the lesion represented in **b** corresponds to the hyper-intense area on the 2-days postoperative MRI and does not include the oedema seen around the lesion (dotted line in **a**). Scale bars: 5 mm in (**a**) and 2 mm in (**b**)

emotional factors, which demanded the interruption of the surgical approach. We also investigated whether the site of the lesion (right, left, or bilateral) was linked to the topographical location of spectral band power changes in the EEG. For that purpose, we calculated spectral band power (12 months after the surgical intervention) in three different regions of interest (ROI). One ROI contained only electrodes from the left scalp part, whereas the second ROI contained only electrodes from the right scalp part. The bilateral ROI contained all electrodes from ROI 1 and 2. Midline electrodes were not included.

EEG recording sessions

Subjects were seated in a dimly lit room shielded against sound and stray electric fields and were video monitored. We recorded a mean of 7.5 min continuous EEG with eyes closed and a mean of 7.5 min continuous EEG with eyes open. Due to the similar results for both experimental conditions, we present here only the results for the eyes closed condition. The recording sessions were performed between 9 to 12 h in order to exclude an impact of circadian factors on the EEG. Subjects were advised to abstain from caffeinated beverages on the day of recording to avoid the caffeine-induced EEG theta decrease (Landolt et al. 2004). Before each recording, subjects were instructed to assume a comfortable position in a chair and were free to place their head on a chin-rest. EEG signals were measured with 60 Ag/AgCl surface electrodes, which were fixed in a cap at the standard positions, according to the extended 10–20 system (M11, Easycap, Herrsching, Germany). During recording, electrode CPz served as reference. Impedance was below 5 kΩ in all electrodes processed for further analysis. Additionally, two bipolar electrode channels were used to monitor eye movements. EEG signals were registered using the SynAmps EEG system (Neuroscan Compumedics, Houston, TX, 0.017 nV precision, sampling rate 250 Hz, 0.3–100 Hz analog band pass filter, -12 dB/octave) and continuously viewed on PC monitor.

Data preprocessing and editing

Data were analyzed offline in Matlab (The Mathworks, Natick, MA) using EEGLAB (http://sccn.ucsd.edu/eeglab/index.html) (Delorme and Makeig 2004). First, the scalp EEG was re-referenced to the mean of the signals recorded at the ear lobes, which was followed by high-pass filtering with a filter of 0.5 Hz to remove linear trends. EEG was visually inspected in 5 s epochs, and eye movement, muscle or heart beat artifacts were removed (mean data length (patients): 5.34 min (± 0.83 min) and mean data length (HC): 5.58 min (± 0.98 min), $p=0.08$, two-tailed two-sample t-test). Next, the EEG was decomposed into independent components using independent component analysis (ICA). After removal of artifact components the signal was reconstructed. The reconstruction of each single ICA component's contribution to the original scalp data is produced by first zeroing out all but the chosen component (row) in the activation matrix, then multiplying by the inverse weight matrix. To investigate the effect of ICA component rejection, we compared patients' (pre-surgery) and HCs' power spectra by two approaches: 1) after visual artifact rejection only (i.e. before ICA) and 2) after additional individual component rejection. Repeated-measures ANOVAs with the factor frequency band power (theta (4–7 Hz), alpha (7–13 Hz), beta (13–30 Hz) and gamma (30–48 Hz)) as within-subject variable and group as between-subject variable revealed no significant difference between the two approaches (delta: $F=0.3$, $p<0.6$; theta: $F=0.3$, $p<0.6$; alpha: $F=0.8$, $p=0.4$; beta: $F=0.002$, $p<0.9$; gamma: $F=0.005$, $p<0.9$). We will hence report only the results of ICA corrected data. We confirmed alertness of subjects during the recording session by checking for slowing of the alpha rhythm, slow rolling eye movements, appearance of alpha spindles or increasing theta power.

Power spectral density

After IC back transformation, spectral analysis was performed on the subjects' average data length (for the eyes closed condition) with the multitaper method that provides a formal method to obtain estimates from the spectrum with optimal bias and variance properties (Mitra and Pesaran 1999). Spectra were calculated with a window length of 5 s, fast Fourier transform (FFT) length of 32 s, and bandwidth parameter nw=2 and $k=3$ tapers (Percival and Walden 1993). Spectral power was log-transformed so that the data distribution was close to the normal distribution (Gasser et al. 1982). The following frequency bands were examined: Low frequency bands: theta (4–7 Hz); middle frequency bands: alpha (7–13 Hz); high frequency bands: beta (13–30 Hz) and gamma (30–48 Hz). To test for significant group differences, the mean band power at each electrode was compared between the particular patient group (HPR and LPR) and the HC group by non-parametric Wilcoxon tests ($p<0.05$, corrected for multiple comparisons using the false discovery rate (FDR) (Benjamini and Hochberg 1995) or $p<0.001$, uncorrected). Results were plotted on topographical maps.

Source analysis

To localize the cortical sources of scalp EEG activity we used low resolution electromagnetic tomography analysis (LORETA; (Pascual-Marqui et al. 1994)). The LORETA method is a discrete, 3D distributed, linear, inverse solution.

The LORETA solution corresponds to the 3D distribution of electrical neuronal activity that features a maximum similarity (i.e. maximum synchronization), in terms of orientation and strength, between neuronal populations in adjacent voxels. The imaging is therefore particularly tuned towards synchronized brain activities as they occur, e.g. in spreading oscillatory activities. Since LORETA takes explicitly into account that scalp electric potentials are determined up to an arbitrary additive constant, the final LORETA solution is independent of the electrical reference used. In the implementation of LORETA, computations were made in a head model using the MNI305 template (Mazziotta et al. 2001), with the three-dimensional solution space restricted to cortical gray matter, as determined by the probabilistic Talairach atlas (Lancaster et al. 2000). Voxel size is 7 mm on each side, i.e. allowing the correct localization of deep structures such as the ACC (Pizzagalli et al. 2001). In addition, this slightly blurry voxel resolution allows a separation of the IC in an anterior and posterior part, since the antero-posterior dimension of the insula is 4–5 cm. In order to calculate tomographic LORETA images we first calculated the cross-spectral density matrix using the multi-taper FFT method. With a spatial over-smoothing of 10^{-4} the current source density was estimated for 2394 cortical voxels within the frequency bands given above. This procedure resulted in one 3D LORETA image for each subject and for each frequency range. LORETA images were statistically compared between groups through multiple voxel-by-voxel comparisons in a nonparametric randomization test (5000 permutations) for functional brain imaging (Nichols and Holmes 2002). All t-values corresponded to $p<0.05$ or $p<0.01$ (corrected for multiple comparisons). The colour coded images are registered to the stereotaxic Talairach space (Talairach and Tournoux 1988), and overlaid onto a MRI template with a scale bar indicating statistical power. Brodmann areas (BA) were used to describe the brain activity pattern.

Correlation analysis

To test for possible pre- and post-operative interactions between the clinical status and EEG activity of the patients, we performed a voxel-wise (whole-brain) correlation analysis. Specifically, activity within each of the 2,394 voxels was correlated with one of the following clinical parameters: pain duration, mean pain intensity, decrease of quality of life, PR and the psychological factors (anxiety, depression, and frustration). In order to compensate for intersubject variability, LORETA maps for each individual were first z-transformed before being entered into the analysis. The statistical threshold for the analysis was set to $p<0.05$, corrected for multiple comparisons using a nonparametric randomization test with 5000 permutations (Nichols and Holmes 2002). For each frequency-band specific p-value we report the according r-value. Although each voxel has its own p-value, subsequent plots will only show (frequency-band specific) significantly correlated voxels at a corrected p-value of $p\leq0.05$.

To test whether treatment resistance was linked to psychological scores, we analyzed PR as a function of the psychological factors, assessed by Pearson's correlations and an analysis of variance (ANOVA) with PR as dependent variable and psychological scores as factors. Further we tested by Pearson's correlations whether PR was linked to the (mean) pain intensity.

Results

According to their postoperative PR, patients were separated in two groups: one group with a high postoperative PR (HPR, $n=14$, PR≥50%), and one group with a low pain relief (LPR, $n=9$, PR<50%). The criterion to split the patients into two groups by 50% PR was justified by previous clinical reports on NP surgery (Kupers and Gybels 1996). Further, a k-mean cluster analysis provides independent statistical support for our proposed split of the continuous variable PR on a clinical basis. Basically, the k-mean cluster analysis represents a method of unsupervised learning and tries to classify a relatively homogeneous group of cases (i.e., NP patients) based on selected characteristics (i.e., PR). The algorithm requires specifying the number of clusters (i.e., two) and performs a distance measure (here: simple Euclidean distance), which will determine the similarity of cases, according to the distance to a particular cluster centre. After normalization of the PR values (Fisher's z-transformation) and 100 iterations as convergence criterion, the analysis revealed two clusters: one cluster with 15 patients (mean PR: 75%) and one with 8 patients (mean PR: 12%). As this analysis yield similar results as obtained by the 50% split criterion, all main results will be presented for the original analysis (HPR, $n=14$ versus LPR, $n=9$).

Pre-CLT EEG results

Across all electrode contacts, we observed a spectral enhancement of the EEG power in different frequency bands in both patient groups (HPR and LPR) as compared to the HC group (Fig. 2a and b). Electrode-wise comparisons revealed significant increases (t-values in a yellow-red color code, with red indicating the strongest statistical differences) for both patient groups, most enhanced in the theta and alpha band (Fig. 2c and d) as compared to the HC group. For the HPR group, fronto-central (FP1-FP1/2, FPz, AFz, AF3/4, AF7/8, Fz, F1/2/3/4/5/6/7, FT7, FC5, FC3,

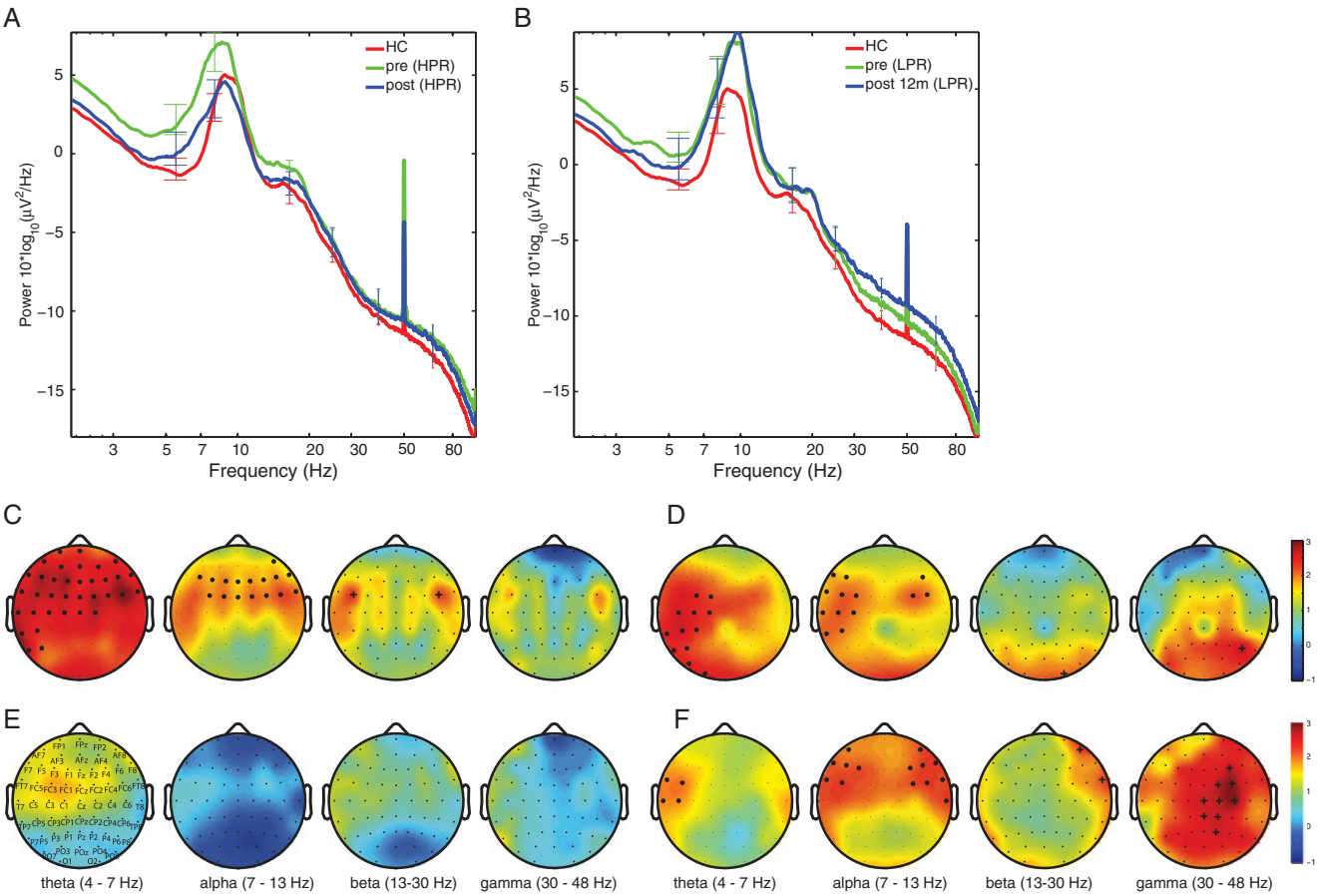

Fig. 2 **a–b** Illustration of resting EEG spectral power distributions across all 60 scalp electrodes for healthy controls (HC, red curves) and neuropathic pain patients, before (*green curves*) and 12 month after (*blue curves*) the central lateral thalamotomy (CLT). **c–f** Topographical distribution of significant frequency-band specific power changes for each of the 60 scalp electrodes (*black dots*) for the HPR and LPR group before (**c** and **b**, respectively) and after the CLT (**e** and **f**, respectively). Electrode names are provided in subfigure E. Significant changes are shown at $p<0.05$ (corrected for multiple comparisons, black dots) or at $p<0.001$ (uncorrected for multiple comparisons, black crosses)

FC1, FCz, and FC2) and temporo-parietal electrodes (TP7, CP5, P7, and P5) showed significantly ($p<0.05$, corrected for multiple comparisons) increased spectral power in the theta band. In the alpha band, fronto-central electrodes (AF8, F5, F3, F1, Fz, F2, F4, F6, F8, FC3, FC1, FCz, FC2, FC4, FC6, and FT8) showed significantly ($p<0.05$, corrected for multiple comparisons) increased spectral power for the HPR than the HC group. In beta, power was only enhanced for the HPR group at FC5 and FC6. For the LPR group, significant ($p<0.05$, corrected for multiple comparisons) increases occurred in left-hemispheric centro-temporal (FC3, FC1, C5, C3, C1, TP7) and parieto-occipital (CP5, CP3, P7, P5, PO7, and O1) electrodes in the theta band. In the alpha band, the LPR group showed significantly ($p<0.05$, corrected for multiple comparisons) increased spectral power compared to the HC group at left-hemispheric fronto-temporal (F7, F5, FT7, T7), fronto-central (FC5, FC3, C5, C3), temporo-parietal (TP7), and centro-parietal (CP5) electrode contacts. On the right hemisphere, spectral power increases were observed at fronto-central (F6, FC4, and FC6) electrodes. In addition, the LPR group showed significant ($p<0.001$, uncorrected) spectral power increases in the beta and gamma band at parieto-occipital (O2 and P6 respectively) electrodes. LORETA revealed that several cortical locations displayed overactivities when the two patients groups were compared to the HC group (Figs. 3 and 4). For clarification, we labeled pain regions on a template brain (Fig. 3a). For the HPR patients, significant overactivities were observed with a left-hemispheric dominance in the theta band bilateral in the IC (BA 13), MCC (BA 24), ACC (BA 24), lateral temporal cortex (lTC, BA 21/22), medial temporal cortex (mTC, BA 20/28/35/36), lPFC (BA 10/46), mPFC (BA 32/6/9/10/11/12), OFC (BA 11/47) and anterior TPC. In alpha and beta overactivities were seen in IC, mTC, lTC, mPFC, ACC and MCC (Fig. 3b–d). Gamma band overactivities (not shown) occurred predominately in the left IC but were not significant.

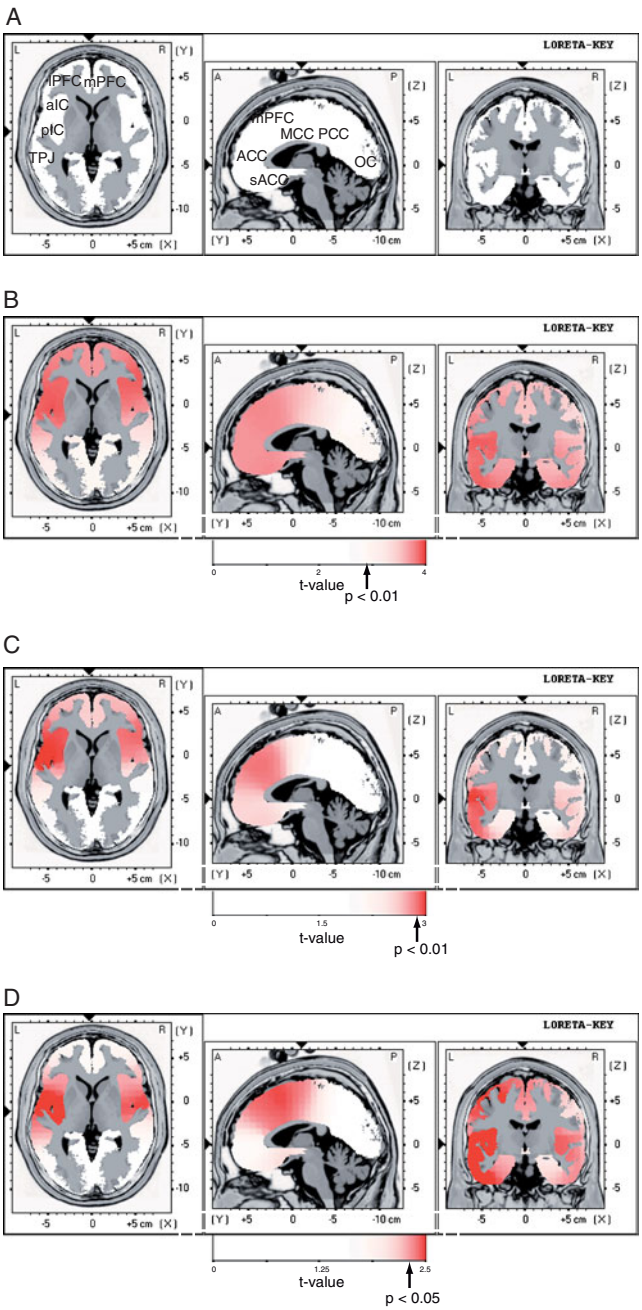

Fig. 3 Illustration of brain regions showing preoperative overactivities for the HPR group. **a** For clarification, main activated areas are labeled on a template brain: *aIC* anterior insular cortex; *pIC* posterior insular cortex; *mPFC* medial prefrontal cortex; *lPFC* lateral prefrontal cortex; *MCC* middle anterior cingulate cortex; *mTC* medial temporal cortex; *ACC* anterior cingulate cortex; *PCC* posterior cingulate cortex; *TPC* temporo-parietal cortex; *ITC* inferotemporal cortex; *OFC* orbitofrontal cortex, and *OC* occipital cortex. The OFC is marked with a blue arrow and extends above the orbita. **b–d** Functional tomographic LORETA maps for the contrast: HPR (pre-surgery) versus HC. For each frequency band, three orthogonal slices are displayed. The color coded images are registered to the stereotaxic Talairach space, and overlaid onto a structural MRI scan. Red areas correspond to overactivities ($p<0.05$ or $p<0.01$, corrected for multiple comparisons; indicated by black arrows) in the HPR group

For the LPR group, overactivities were observed, with a left dominance too, in the IC and MCC in the theta and alpha band (Fig. 4a–b). However, in contrast to the HPR group, activities were more pronounced in the pIC (BA 13), adjacent temporo-parietal cortex (TPC, BA 21/22), lTC, mTC and lPFC. Beta and gamma overactivities were found in the occipital cortex (OC, BA 17/18/19/37), IC (beta only) and TPC (beta only), as shown in Fig. 4c–d.

Additionally, we tested the reliability of the source localization results with a more rigorous way to split the two patients groups. Here we used 11 patients of the HPR group (PR≥70%) and 8 patients of the LPR group (PR≤ 30%).The results demonstrated a high similarity, i.e. a high spatial overlap of overactivities at similar statistical thresholds between this and our original analysis (data not shown).

We also tested the relevance of pain location for both groups, i.e. we compared brain activities for patients with trigeminal and without trigeminal pain (i.e., 9 versus 5 patients in the HPR group and 3 versus 6 patients in the LPR group). The results are shown in Fig. 5. For both patient groups, we did not find significant differences for any frequency band. There was only a trend for stronger beta band activity for HPR patients with trigeminal pain.

Pre-CLT EEG/clinical results

The whole-brain correlation analysis across both patient groups revealed significant (theta: $p<0.05$, $r=0.44$; beta: $p<0.05$, $r=0.43$) interactions or a trend (alpha: $p<0.1$, $r=0.32$) between the mean pain intensity and EEG activity in the cingulate, prefrontal, orbitofrontal and insular areas as illustrated in Fig. 6a. Specifically, correlations in theta were located in PCC, left IC, and OC; in alpha in the ACC, MCC, mPFC, lPFC and left IC; in beta in ACC, lPFC, mPFC and OFC. Frustration was positively correlated with EEG activity in the ACC, MCC, IC, mPFC, lPFC and OFC (theta: $p<0.05$, $r=0.36$) as shown in Fig. 6b.

Post-CLT EEG results

Twelve months after CLT we found, as compared to the HC group, that the HPR group had a normalized spectral power (Fig. 2a). Electrode-wise comparison revealed that this normalization was visible in all frequency bands and in all electrodes as shown in the topographical maps of Fig. 2e. In contrast, spectral band power for the LPR group remained enhanced in low and especially in high frequency bands compared to the HC group (Fig. 2b). Electrode-wise comparison showed significant ($p<0.05$, corrected for multiple comparisons) spectral power increases in theta at left fronto-temporal (FT7, T7), fronto-central (FC5), and central (C5) electrodes. For alpha, spectral power increases

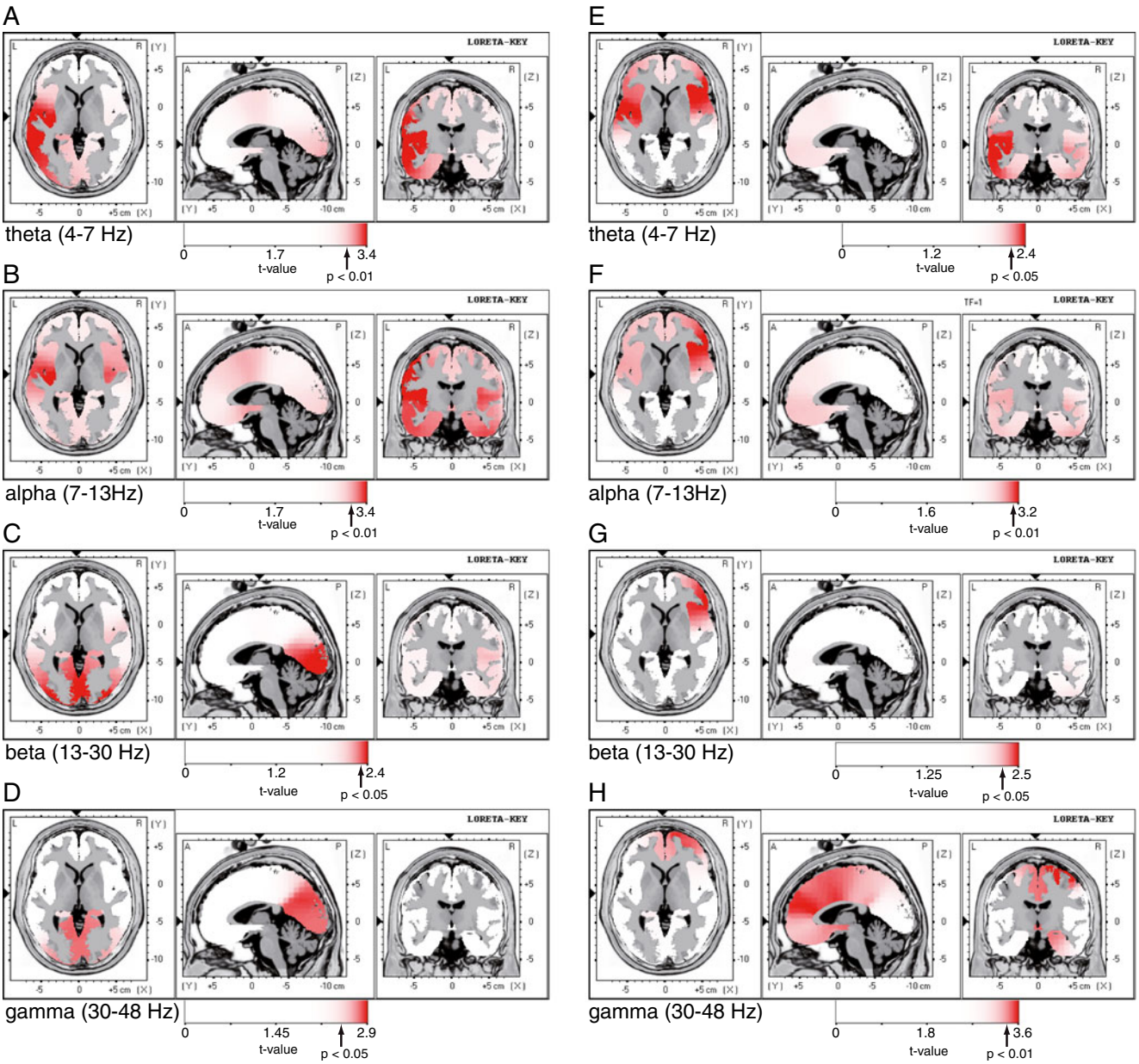

Fig. 4 Functional tomographic LORETA maps for the contrast LPR (pre-surgery: **a–d** and 12 month post-surgery: **e–h**) versus HC. Red areas correspond to overactivities ($p<0.05$ or $p<0.01$, corrected for multiple comparisons; indicated by *black arrows*)

at the same statistical threshold were observed bilaterally at frontal (AF7, AF8, F7, F5, F3, F4, F6, F8), left fronto-temporal (FT7 and FT8), bilateral fronto-central (FC5, FC4, and FC6), and left temporal (T8) electrodes. In beta, spectral power increases ($p<0.001$, uncorrected) occurred at right frontal (AF8) and left fronto-temporal (FT8) electrodes. In gamma, significant ($p<0.001$, uncorrected) spectral power increases were seen at right frontal (F4), fronto-central (FC2 and FC4), central (Cz, C2, and C4), and centro-parietal (CPz, CP2, and P2) electrodes (2 F).

LORETA results are presented in two ways. First, we compared each of the patient groups (12 months after surgery) to the HC group (*contrast 1*). Second, we calculated within-group comparisons, comparing the EEG activity patterns before and 12 months after CLT for each of the two patient groups (*contrast 2*). For contrast 1 we found that there were no significant overactivities visible for the HPR group, irrespectively of the investigated frequency band (all $p>0.1$, data not shown). For the LPR group we observed two findings (Fig. 4e–h). First, significant overactivities were visible in all frequency bands. Second, these overactivities were located in the IC, lPFC, mPFC, MCC, ACC, PCC and OFC. We observed, comparing with the pre-operative state, a switch from

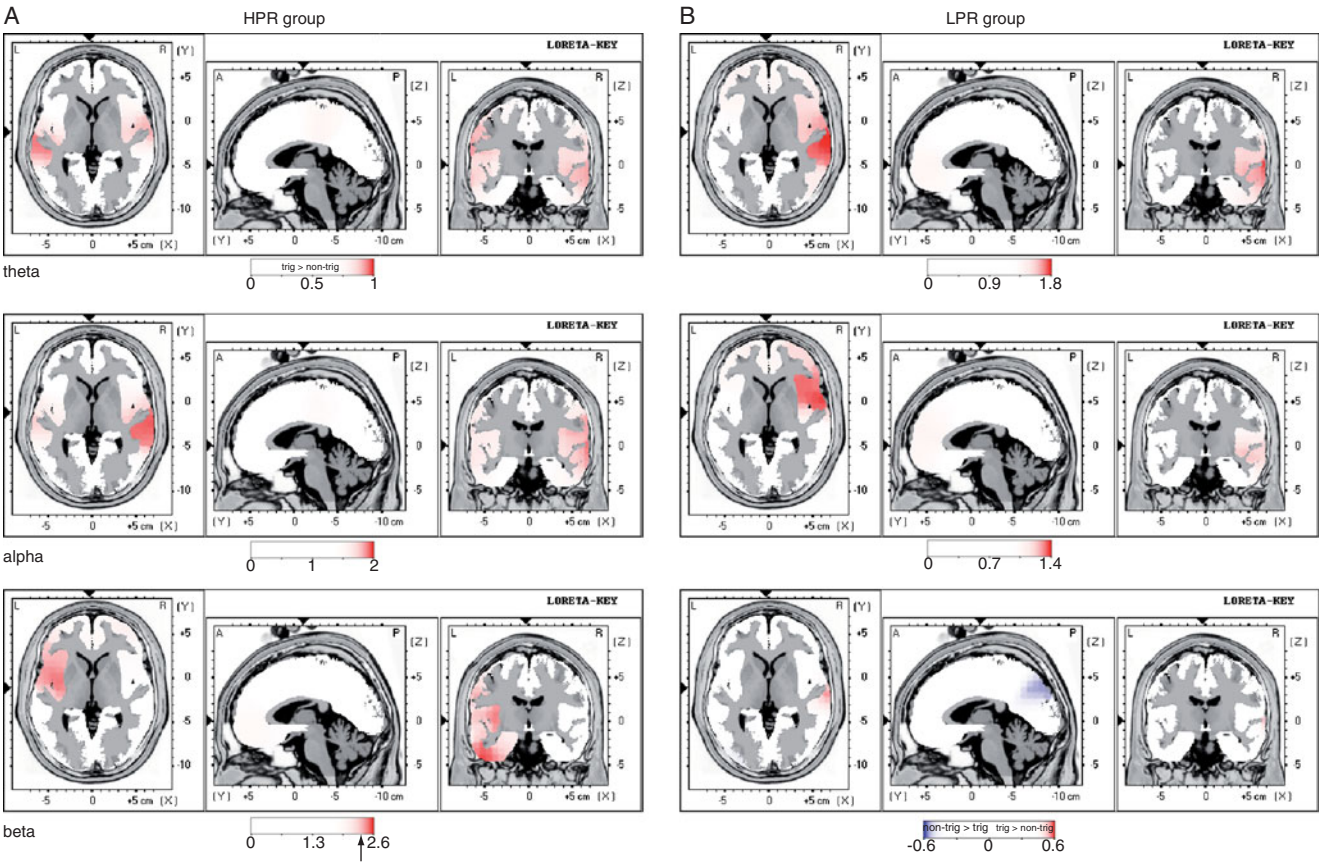

Fig. 5 Illustration of (pre-surgery) brain activation differences between HPR **(a)** and LPR **(b)** patients with trigeminal and without trigeminal pain. Red areas indicate regions in which patients with trigeminal pain showed stronger EEG activations than patients without trigeminal pain. None of the comparisons reached statistical significance. The black arrow indicates the threshold for a statistical trend ($p<0.1$)

posterior to anterior and from left to right regions, i.e. from the left pIC and TPC to the right aIC and lPFC.

Contrast 2 revealed for the HPR group (Fig. 7a and b) alpha and beta pre-CLT overactivities (red color code) as compared to the post-CLT state in the IC, ACC, MCC, lTC, mTC, mPFC, lPFC and TPC similar to what was seen in the comparison with HC, indicating that the obtained post-CLT reductions were well centered on the overactive pre-CLT areas. For the LPR group (Fig. 7c and d), significant right-dominant alpha and beta overactivities were seen in the post-CLT condition (blue colors) as compared to the pre-CLT state, which are located in the lPFC, mPFC, aIC and ACC. This result parallels the findings from contrast 1 and further indicates that HPR and LPR patients showed different postoperative brain activity patterns.

As the HPR group did not show overactivities anymore 12 months after the CLT compared to HC group, we additionally tested whether the contrast 'LPR versus HPR' leads to similar result as the contrast 'LPR versus HC. Indeed, we found that the LPR group show significant right-hemispheric overactivities in the insular and orbito-frontal cortex in the alpha and beta band. For theta and gamma, overactivities are visible at the right insular cortex and the medial PFC but failed to reach significance (Fig. 7e). This can be most probably explained by the fact (12 months post-surgery) spectral band power was not fully normalized in the HPR group (Fig. 2a).

Further, we did not find an effect on spectral band power related to the side of the lesion (Fig. 8). For example, a unilateral lesion (left or right) revealed similar spectral band power (1–48 Hz) in the three different ROIs, and was thus not linked to the side of the lesion.

Post-CLT EEG/clinical results

A comparison of the post-CLT clinical results between both groups revealed significantly higher (mean) pain intensity values as well as higher psychological scores (trend for anxiety) for the LPR group compared to the HPR group. In addition, decreases in quality of life were significantly higher for the LPR group. Further, PR was significantly negatively correlated to (mean) pain intensity across all patients ($r=-0.75$, $p<0.0001$), Table 2 provides detailed information about the individual test scores for each patient before and after surgery. The whole-brain correlation

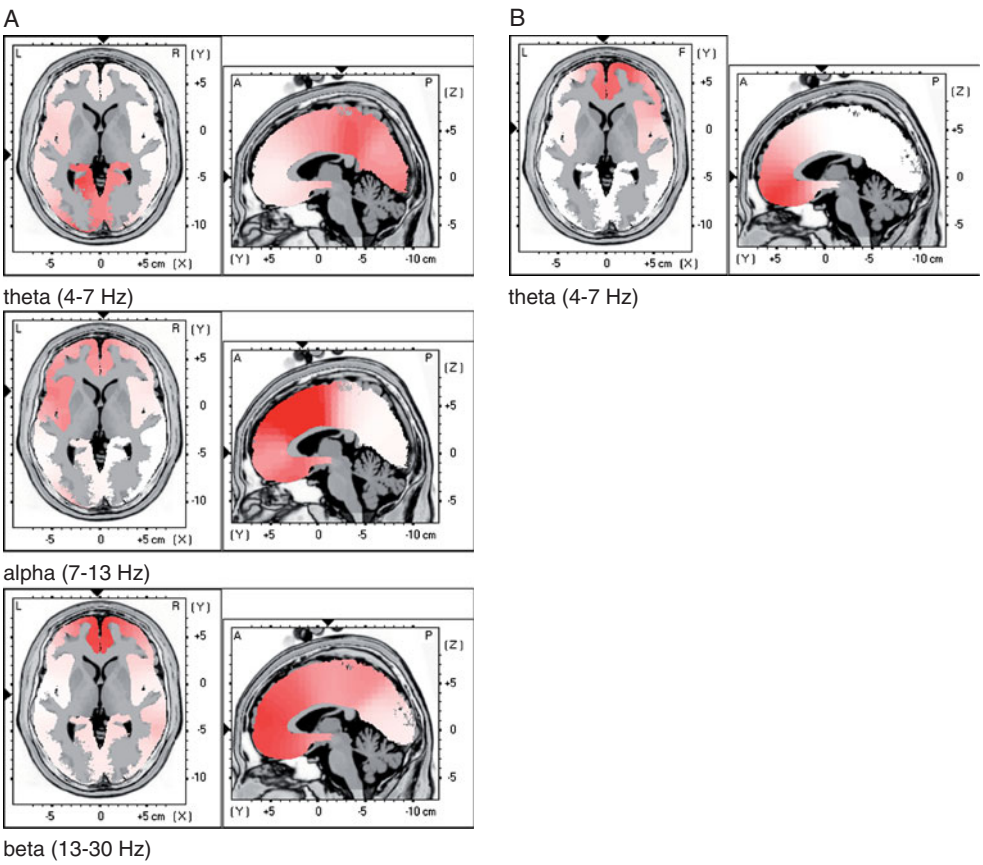

Fig. 6 Pre-surgery whole brain correlation analysis between the factors pain intensity (**a)** or frustration (**b)** and LORETA EEG activity averaged for the HPR and LPR groups

analysis for the HPR group revealed that PR was negatively correlated with EEG activities in ACC, MCC, IC, mPFC, lPFC, PCC, TPC and OFC (theta: $p<0.01$, $r=-0.5$; alpha: $p<0.01$, $r=-0.64$; beta: $p<0.01$, $r=-0.78$) as shown in Fig. 9a. For the LPR group, frustration was positively correlated with lPFC, ACC, mPFC, IC and OFC activity (theta: $p<0.05$, $r=0.45$) as shown in Fig. 9b.

Across all patients, an ANOVA with PR as dependent variable and the psychological factors (frustration, depression, anxiety) as predictor revealed a trend ($F=2.94$, $p<0.057$). Further, PR was significantly negatively correlated to *all* psychological factors (Pearson correlations, all $p<0.002$).

Although it has been demonstrated that medication has an effect on the EEG, it was shown recently that spectral power and source localization differences between medicated and non-medicated chronic NP patients are small (Stern, et al. 2006). However, we additionally examined the influence of medications on the postoperative brain activity by comparing the source localization results of six HPR patients with medication to eight HPR patients without medication. Only in the theta band elevated ($p<0.1$) activity was observed for the medicated group within the mPFC, ACC, and IC (not shown).

As some of the HPR and LPR patients show a PR of 50% or close to 50% (4 patients in with a PR between 40% and 70%), we additionally tested whether the pre- and post-surgery results of the source localization analysis are comparable if we exclude the described four patients. Thus, we compared 11 HPR (PR≥70%) patients and 8 LPR (PR≤40%) patients to 15 HC respectively, and found highly comparable results to our original analysis (e.g., same statistical threshold and similar spatial locations of overactivities).

Discussion

Preoperative observations

We could first confirm on a larger patient group the results of EEG studies on NP (Sarnthein et al. 2006; Stern et al. 2006). NP patients display before treatment a robust increase of their EEG power spectra in broad low and high frequency bands. The source localization of these EEG overactivities is centered in the cortical NP matrix, mainly in IC, cingulate areas and mPFC. Another complementary way to demonstrate such a causal relationship has been to correlate EEG overactivities with pain intensity. This was obtained by applying a whole-brain voxel-to-voxel procedure, which evidenced a significant correlation between pain intensity and cingulate and mPFC overactivities. These

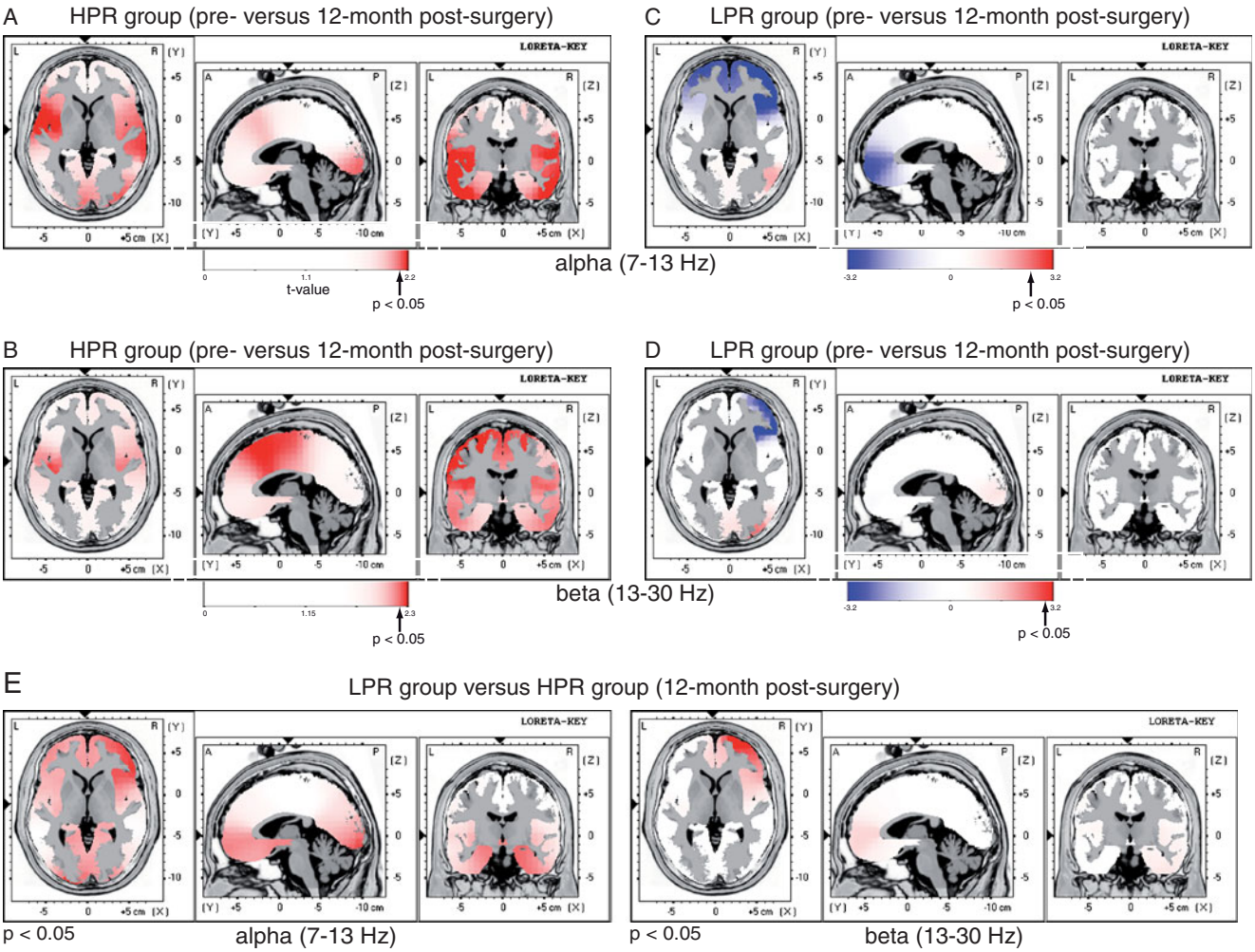

Fig. 7 Functional tomographic LORETA maps for the contrast pre- versus post surgery for the HPR group **(a, b)** and the LPR group **(c, d)** as well as 12-month post-surgery contrast 'LPR group versus HPR group' (**e**). The red color code in **a–d** indicates stronger activation before than after the surgery; the blue color code indicates stronger activation after than before the surgery. The red color code in **e** indicates stronger activation for the LPR than the HPR group. All results are displayed at $p<0.05$ (corrected for multiple comparisons)

results are in line with the well-known central role of cingulate and PFC areas during experimental pain and NP (Apkarian et al. 2001, 2005; Baliki et al. 2006; Ballantine et al. 1967; Dube, et al. 2009; Hsieh et al. 1995; Jones et al. 2003a; Peyron et al. 2000; Ploner et al. 2002; Salomons et al. 2007; Sarnthein et al. 2006; Starr et al. 2009; Stern et al. 2006; Treede et al. 1999, 2003; Wager et al. 2004; Willoch et al. 2000). It is also known that the unpleasantness of pain activates the cingulate and PFC (Mobascher et al. 2009), amygdala, and insula (Brooks et al. 2005), although all of these studies examined exogenously induced pain (e.g., induced by painful stimulation) rather than chronic NP. The key structure of the medial pain system is the ACC, which is a functionally heterogeneous brain area that receives its main afferents from the medial thalamic nuclei and which has been implicated in the integration of cognition, affect and social behaviour (Devinsky et al. 1995). The largest evidence for the coupling of cingulate areas and pain processing came from lesion and stimulation studies (Ballantine et al. 1967; Spooner et al. 2007). Specifically, it has been shown that cingulotomy provides significant PR in half to three quarters of pain patients (Ballantine et al. 1967). Recently, it has been demonstrated in a patient with phantom limb pain treated with deep brain stimulation (DBS) that pain-related activities were found in the IC, OFC and ACC areas (Kringelbach et al. 2007). Our data are fully in line with these observations.

One might ask whether the HPR and LPR group show already spectral band power or localization differences before the operation. This question is highly significant in the search for the possibility of a pre-treatment selection of the patients who will benefit from surgery. However, Fig. 10 demonstrates that the two groups cannot be separated at the pre-surgical level. Further studies on larger groups will hopefully provide statistical evidence for such a separation.

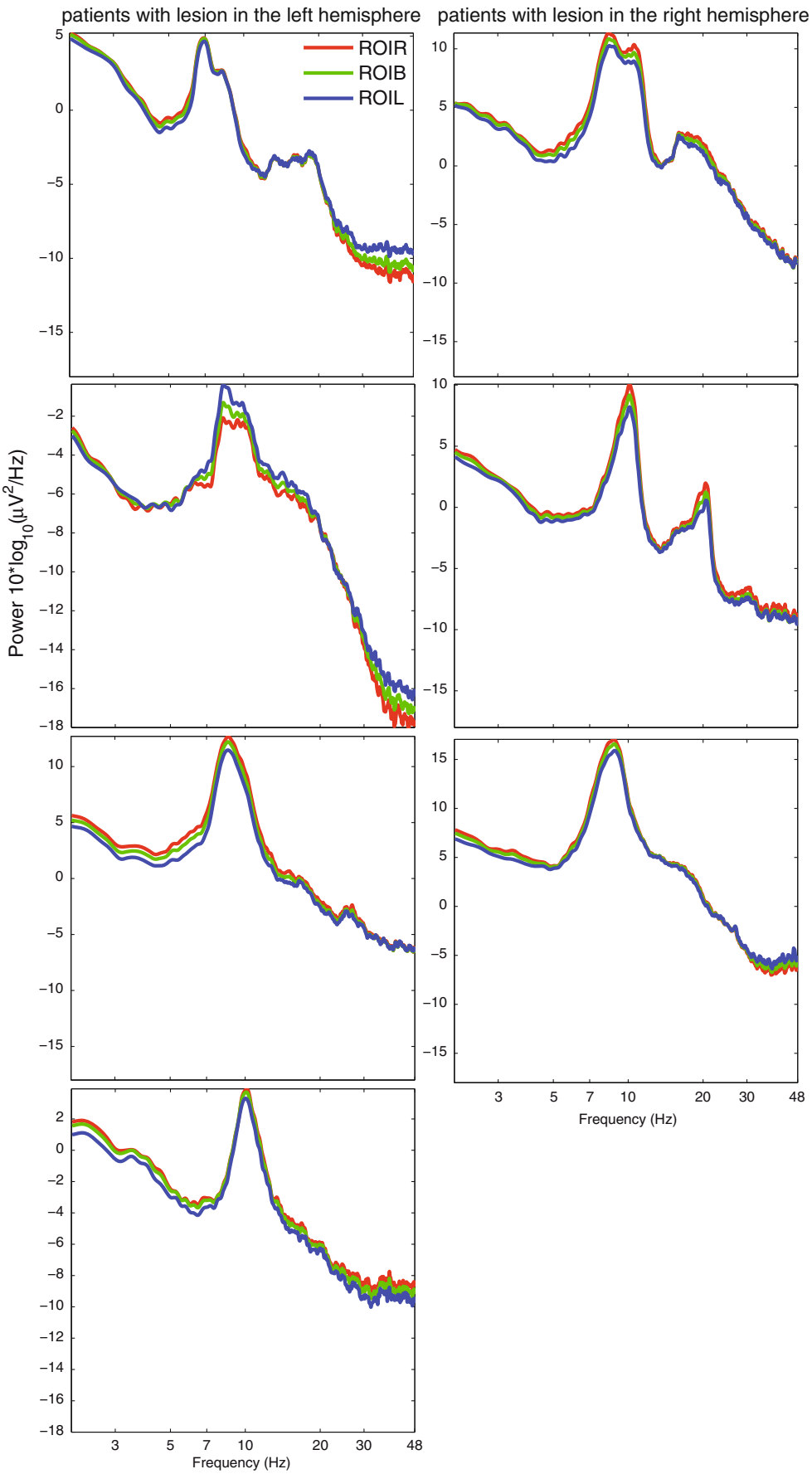

Fig. 8 Illustration of spectral EEG band power differences (12 month after the surgical intervention) for three different regions of interests in patients with a unilateral lesion (right or left hemisphere). The red line in each panel shows the average spectral band power (1–48 Hz) for electrodes of the right scalp (ROIR). The green line in each panel represents average spectral band power for all electrodes (ROIB). The blue line in each panel shows the average spectral band power for electrodes of the left scalp (ROIL). For all ROIs, midline electrodes were not included

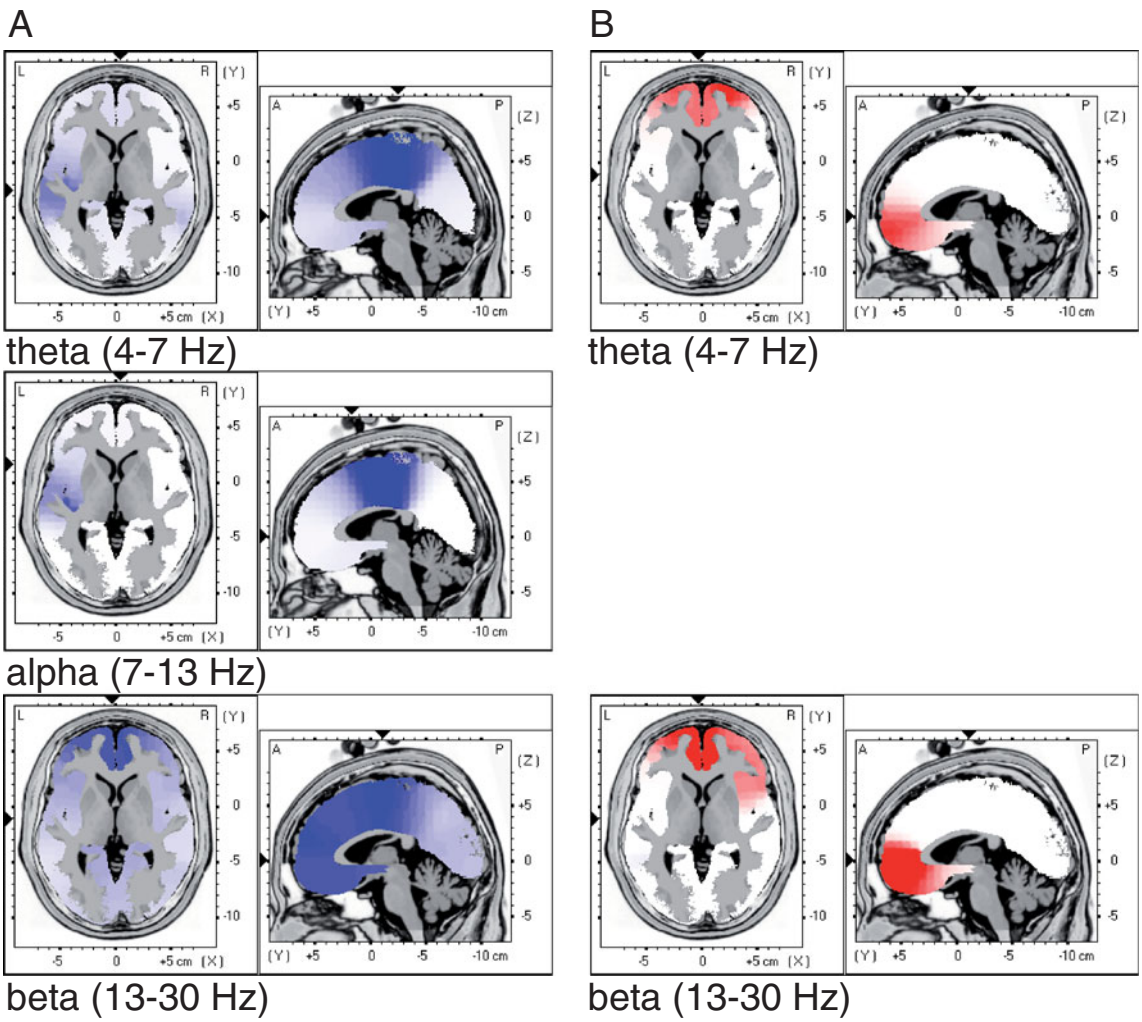

Fig. 9 Illustration of the post-surgery results for whole brain correlation analysis between the factors pain relief (**a**) and frustration (**b**) and LORETA EEG activity. For pain relief, the correlations analysis is performed only for the HPR group; for frustration, it is performed only for the LPR group

Postoperative operations: treatment resistance

Postoperatively, the HPR group demonstrates a normalization by the CLT of both power spectrum and source localization. A confirmation of such an effect comes through the whole-brain voxel-to-voxel analysis, which demonstrates an inverse correlation between PR and activity in the cingulate areas, OFC, PFC and IC, as well as between PR (across all patients) and psychological factors (anxiety, depression and frustration).

To the contrary, we observed no normalization of EEG parameters in CLT-resistant patients (LPR group). One might ask whether a low PR could be explained by a failure in the CLT procedure itself. However, this can be excluded by the postoperative reconstruction of all CLTs in this study. These were indeed included based on their millimeter level reconstruction showing them to be on target (Fig. 1).

Most interestingly, the remaining overactivities shifted from left posterior to right anterior cortical areas, centered on prefrontal, insular, cingulate and orbitofrontal regions. Thus, our study demonstrates complex bilateral EEG effects, which do not correlate with the pain lateralization (see Table 1). Central yet unidentified factors are thus to be envisaged, which might explain this shift from preoperative left-dominance to postoperative right dominance. This might be attributed to differentially lateralized prefrontal emotional coding (Budell et al. 2010; Peyron et al. 2000a). The shift of EEG overactivity from the posterior to the anterior IC might be explained by its key role in mediating human awareness (Craig 2009) and by its involvement in mediating the influence of cognition on pain, i.e. when subjects have to estimate their experience of pain (Kong et al. 2006).

The postoperative correlation of the frustration score with EEG activities in ACC, IC, PFC and OFC in the LPR

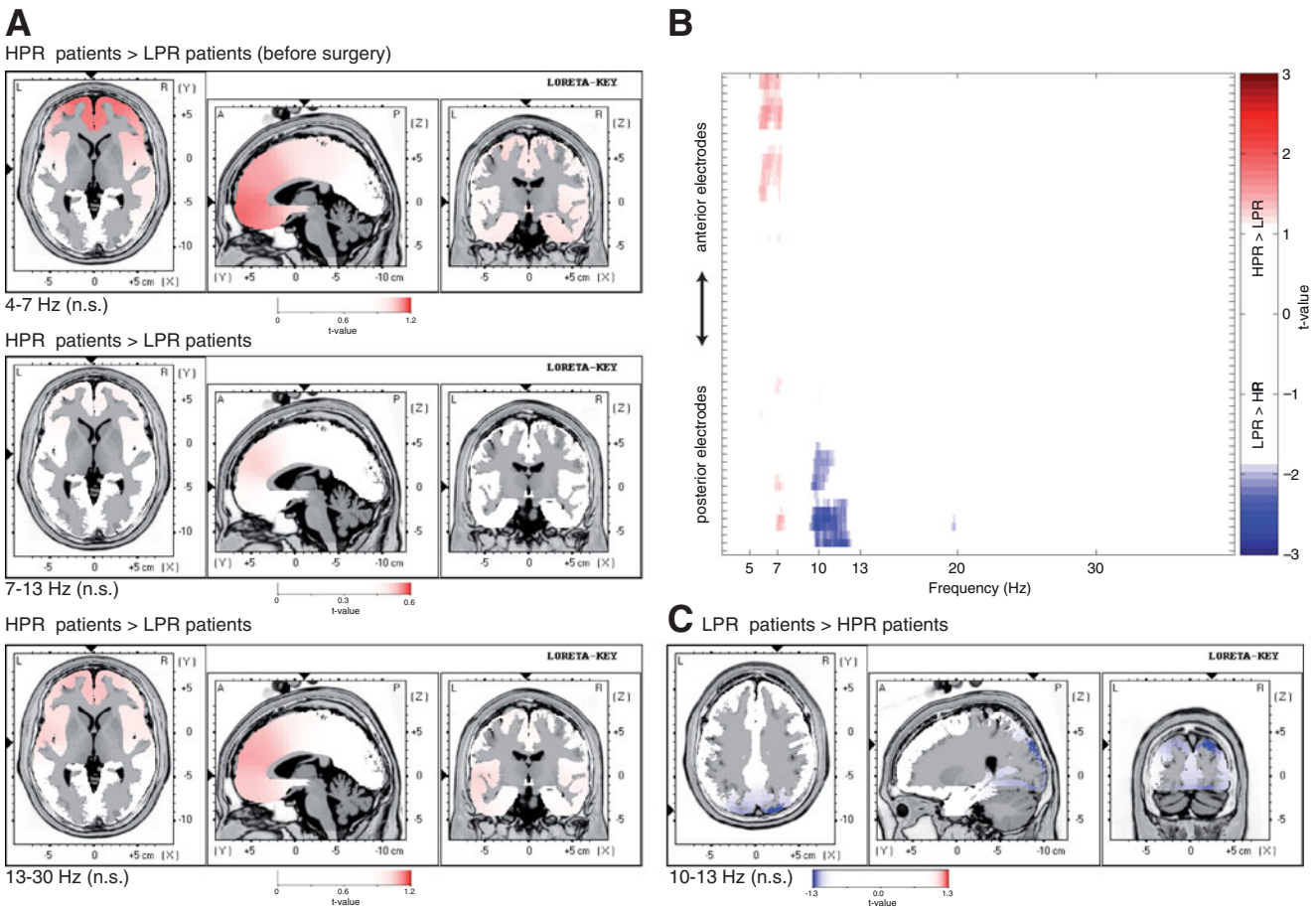

Fig. 10 Illustration of EEG activity (**a, c**) and spectral EEG band power (**b**) differences for the pre-surgical contrast 'HPR versus LPR' and 'LPR versus HPR'. Red areas in **a** indicate regions in which HPR patients exhibited stronger brain activity than LPR patients. Red areas in **b** reflect electrode locations that showed higher spectral band power for HPR than LPR patients. Blue regions in **c** indicate regions in which LPR patients exhibited stronger brain activity than HPR patients. The only significant group differences were seen at a few parieto-occipital electrodes in the alpha band (**b**)

group indicates an association of this feeling with the occurrence of a resistance to therapy. As mentioned above, it is known that emotional-cognitive functions, including the integration of the affective-emotional aspect of pain, are represented in the cingulate, but also insular and frontal regions (Brooks et al. 2005; Chen et al. 2008; Herwig et al. 2010; Nielen et al. 2009; Northoff et al. 2000). Because the pain and the paralimbic-associative networks overlap subtotally, our study cannot claim to separate pain-related and cognitive/emotional phenomena. And because emotions are used exclusively in correlation analyses with EEG data, we cannot propose for them a causal relationship with cortical events. Indeed, it remains to be demonstrated if therapy-resistance happened because of a particularly counterproductive frustration dynamics, or if frustration remained high postoperatively because surgery could not reduce pain sufficiently due to other factors still to be identified.

Pathophysiological mechanisms for NP

Several mechanisms have been proposed for the pathophysiology of NP (Apkarian et al. 2005; Jones et al. 2003b; Llinás et al. 1999; Peyron et al. 2000b; Treede et al. 1999). Among them, it has been argued that NP relies on disturbed thalamocortical interactions, known as thalamocortical dysrhythmia (Llinas et al. 1998, 1999), for which a computational model was presented recently (Proske et al. 2011). Thalamic microelectrode recordings have shown the presence of low threshold calcium spike (LTS) bursts in the somatosensory (Lenz et al. 1989) and medial (Jeanmonod et al. 1993; 1996) thalamus of NP patients. LTS bursts displayed low frequency (theta) rhythmicity, with a mean interburst discharge rate of 4 Hz. These bursts were described in vitro and in vivo and related to a state of membrane hyperpolarization (Llinás and Jahnsen 1982; Steriade et al. 1997). This enhanced theta thalamic activity

found a correlate in local field potentials, EEG and MEG studies (Llinás et al. 1999; Moazami-Goudarzi et al. 2010; 2008; Sarnthein and Jeanmonod 2008; Sarnthein et al. 2006; Schulman et al. 2005; Stern et al. 2006). Evidence for the role of the medial thalamus in NP came already from clinical studies in the late forties (Hécean et al. 1949), since it was demonstrated that in contrast to all other lesional surgeries, medial thalamotomies against NP provide a good success rate, produce no somatosensory or other deficits, and have a low complication rate, with especially the absence of risk for the development of iatrogenic pain (Jeanmonod et al. 1994; Jeanmonod and Morel 2009; Sano 1977). This relevance of the medial thalamus in NP is supported by the anatomical connectivity of CL, which relays pain information, conveyed mainly through the spinothalamic tract, to a large number of the areas involved in NP, including S2, IC, ACC, OFC and PFC (Apkarian and Shi 1994; Craig 1996; Willis 1985; Willis and Westlund 1997).

Limitations

A limitation of our study might be that EEG LORETA source localization does not provide a high spatial resolution such as fMRI. Nevertheless our results reveal three important findings: first, we replicate not only EEG and MEG findings (Stern et al. 2006) but also other functional brain imaging studies of chronic NP processing (Apkarian et al. 2001; Hsieh et al. 1995). In addition, we found two important differences between patient groups: first, the absence of post-operative overactivities in the HRP group, and second, the remaining significant post-surgical overactivities for the LPR group, with a shift from left and posterior (pre-surgery) to right and anterior hemispheric localization. This shift could be clearly detected with LORETA source localization. In addition, the different pre- and post-surgery EEG activity patterns could be resolved satisfactorily: for example, the voxel size is 7 mm, i.e. is much smaller than the antero-posterior spatial extent (4–5 cm) of the IC, in which we observed differential posterior and anterior localizations. In fact, the LORETA EEG source localization seems to be most appropriate for the analysis of a widespread and distributed bi-hemispheric process like NP.

In various commonly used instruments, such as the Hamilton Depression and Anxiety questionnaires (HAMD and HAMA), the 0–4 rating scale is used as basis because it can be easily implemented by the patients and provides a sufficient level of differentiation. These questionnaires use the sum of many 0–4 rating scales. Frustration has been much less examined: there exists no well recognized frustration scale, and the few instruments at disposition address specific sub-issues of no direct interest to this study, e.g. anger expression (STAXI-2), reaction to frustration (RFS), or frustration intolerance and discomfort (FDS). To obtain a homogeneous analysis of depression, anxiety and frustration and to facilitate correlation analyses, we chose to rate these three items in a simplified way, based only on one single 0–4 scale each. This simplification represents a significant limitation of this study.

The functional significance of EEG frequency bands in pain perception

Our results indicate that different brain regions demonstrate NP-related activity in multiple EEG frequency bands. Our correlation analyses complement the evidence collected from comparisons between patient and control groups, to demonstrate the relevance of an EEG frequency-based approach in the understanding of NP mechanisms. Specifically, we suggest that the link between frustration and theta activity (in the ACC, PFC, and IC) underlines the role of low-frequency activity not only as a marker for NP (see pre-surgical results) but also as a marker for treatment resistance. Otherwise, the correlation between post-operative frustration values and theta-related activity should not be seen. In contrast, PR is linked in a much broader fashion to oscillatory activity than frustration, because the observed correlations with PR were seen in low, middle, and higher frequency bands. Our study could demonstrate for the first time that this coupling is linked to predominant overactivities in the IC, ACC, and MCC. During real-time fMRI it has been shown that individuals who could control ACC activity (via visual feedback) during experimentally induced pain reported less pain (deCharms et al. 2005). We suggest that ACC and potentially IC and MCC are further partners which are linked to suffering (e.g., manifested by PR and frustration), and that the degree of suffering is directly coupled to oscillatory activity (Figs. 6 and 9). Neurofeedback training, e.g. controlling brain oscillatory activity through visual feedback, might help to further enhance PR in (treated and untreated) NP patients.

It is known that an altered functionality within the PFC (as also seen in this study) is linked to structural loss within this area in NP patients (May 2008). Thus, we cannot exclude that EEG frequency power differences between the LPR and HPR group might be related to differences in cortical reorganization.

We show in addition that the dysrhythmic process at the source of NP affects both hemispheres in spite of the presence of unilateral pain, and that EEG spectral power does not show lateralization effects after unilateral therapeutic lesions. Quantitative EEG studies have also been useful in the different though neighbour field of induced, nociceptive pain. Alpha activity in sensorimotor cortical

areas was seen contralateral to the side of the induced pain, while beta activity was linked to changes in the ipsilateral hemisphere (Stancak et al. 2007). Both EEG power and EEG peak frequency were related to nociceptive pain stimulation. For example, it was shown that tonic noxious stimulation was positively linked to the alpha peak frequency – a marker for attention demands, cognitive performance, arousal, and potentially a marker for a personal signature (Klimesch et al. 1990; Napflin et al. 2007) – at bilateral temporal recording sites (Nir et al. 2010).

Conclusion

The observed normalization of both power spectrum and source localization speaks for a selective regulation by CLT of a dysfunctional thalamocortical system. Our results, however, also underlines the importance of the human cognitive/emotional domain, able to jeopardize this normalizing effect. This is consistent with the size of the paralimbic/associative network, which codes for concepts and emotions in the human brain, and with the imbedding of the pain matrix inside this network. Our results point in addition to the relevance of a frustration-based dynamics in chronic NP. They emphasize the absolute necessity to integrate surgical and psychotherapeutic approaches, and might be useful in a search for further adaptations of both therapeutic options in these difficult chronic situations.

Acknowledgments We thank J. Sarnthein and J. Dodd for help with the EEG recordings, and A. Morel for helpful comments on earlier versions of the manuscript.

References

Apkarian, A. V., & Shi, T. (1994). Squirrel monkey lateral thalamus. I. vSomatic nociresponsive neurons and their relation to spinothalamic terminals. *Journal of Neuroscience, 14*(11 Pt 2), 6779–6795.

Apkarian, A. V., Thomas, P. S., Krauss, B. R., & Szeverenyi, N. M. (2001). Prefrontal cortical hyperactivity in patients with sympathetically mediated chronic pain. *Neuroscience Letters, 311*(3), 193–197.

Apkarian, A. V., Bushnell, M. C., Treede, R. D., & Zubieta, J. K. (2005). Human brain mechanisms of pain perception and regulation in health and disease. *European Journal of Pain, 9*(4), 463–484.

Baliki, M. N., Chialvo, D. R., Geha, P. Y., Levy, R. M., Harden, R. N., Parrish, T. B., et al. (2006). Chronic pain and the emotional brain: Specific brain activity associated with spontaneous fluctuations of intensity of chronic back pain. *Journal of Neuroscience, 26*(47), 12165–12173.

Ballantine, H. T., Jr., Cassidy, W. L., Flanagan, N. B., & Marino, R., Jr. (1967). Stereotaxic anterior cingulotomy for neuropsychiatric illness and intractable pain. *Journal of Neurosurgery, 26*(5), 488–495.

Benjamini, Y., & Hochberg, Y. (1995). Controlling the False Discovery Rate: A Practical and Powerful Approach to Multiple Testing (Vol. 57, pp. 289–300): Blackwell Publishing for the Royal Statistical Society.

Bingel, U., Quante, M., Knab, R., Bromm, B., Weiller, C., & Buchel, C. (2002). Subcortical structures involved in pain processing: evidence from single-trial fMRI. *Pain, 99*(1–2), 313–321.

Boord, P., Siddall, P. J., Tran, Y., Herbert, D., Middleton, J., & Craig, A. (2008). Electroencephalographic slowing and reduced reactivity in neuropathic pain following spinal cord injury. *Spinal Cord, 46*(2), 118–123.

Bornhovd, K., Quante, M., Glauche, V., Bromm, B., Weiller, C., & Buchel, C. (2002). Painful stimuli evoke different stimulus-response functions in the amygdala, prefrontal, insula and somatosensory cortex: a single-trial fMRI study. *Brain, 125*(Pt 6), 1326–1336.

Brooks, J. C., Zambreanu, L., Godinez, A., Craig, A. D., & Tracey, I. (2005). Somatotopic organisation of the human insula to painful heat studied with high resolution functional imaging. *NeuroImage, 27*(1), 201–209.

Buchel, C., Bornhovd, K., Quante, M., Glauche, V., Bromm, B., & Weiller, C. (2002). Dissociable neural responses related to pain intensity, stimulus intensity, and stimulus awareness within the anterior cingulate cortex: a parametric single-trial laser functional magnetic resonance imaging study. *Journal of Neuroscience, 22*(3), 970–976.

Budell, L., Jackson, P., & Rainville, P. (2010). Brain responses to facial expressions of pain: Emotional or motor mirroring? *NeuroImage, 53*(1), 355–363.

Chanda, M. L., Alvin, M. D., Schnitzer, T. J., & Apkarian, A. V. (2011). Pain characteristic differences between subacute and chronic back pain. *J Pain*.

Chen, F. Y., Tao, W., & Li, Y. J. (2008). Advances in brain imaging of neuropathic pain. *Chinese Medical Journal (Engl), 121*(7), 653–657.

Craig, A. D. (1996). An ascending general homeostatic afferent pathway originating in lamina I. *Progress in Brain Research, 107*, 225–242.

Craig, A. D. (2009). How do you feel–now? The anterior insula and human awareness. *Nature Reviews Neuroscience, 10*(1), 59–70.

deCharms, R. C., Maeda, F., Glover, G. H., Ludlow, D., Pauly, J. M., Soneji, D., et al. (2005). Control over brain activation and pain learned by using real-time functional MRI. *Proceedings of the National Academy of Sciences of the United States of America, 102*(51), 18626–18631.

Delorme, A., & Makeig, S. (2004). EEGLAB: an open source toolbox for analysis of single-trial EEG dynamics including independent component analysis. *Journal of Neuroscience Methods, 134*(1), 9–21.

Devinsky, O., Morrell, M. J., & Vogt, B. A. (1995). Contributions of anterior cingulate cortex to behaviour. *Brain, 118*(Pt 1), 279–306.

Downar, J., Crawley, A. P., Mikulis, D. J., & Davis, K. D. (2002). A cortical network sensitive to stimulus salience in a neutral behavioral context across multiple sensory modalities. *Journal of Neurophysiology, 87*(1), 615–620.

Downar, J., Mikulis, D. J., & Davis, K. D. (2003). Neural correlates of the prolonged salience of painful stimulation. *NeuroImage, 20*(3), 1540–1551.

Dube, A. A., Duquette, M., Roy, M., Lepore, F., Duncan, G., & Rainville, P. (2009). Brain activity associated with the electrodermal reactivity to acute heat pain. *NeuroImage, 45*(1), 169–180.

Garcia-Larrea, L., Frot, M., & Valeriani, M. (2003). Brain generators of laser-evoked potentials: From dipoles to functional significance. *Neurophysiologie Clinique, 33*(6), 279–292.

Gasser, T., Bächer, P., & Möcks, J. (1982). Transformations towards the normal distribution of broad band spectral parameters of the EEG. *Electroencephalography and Clinical Neurophysiology, 53*(1), 119–124.

Hécean, H., Talairch, J., David, M., & Dell, M. (1949). Coagulations limitées du thalamus dans les algies du syndrome thalamique. *Revista de Neurologia, 81*, 917–931.

Herwig, U., Kaffenberger, T., Jancke, L., & Bruhl, A. B. (2010). Self-related awareness and emotion regulation. *NeuroImage, 50*(2), 734–741.

Hsieh, J. C., Belfrage, M., Stone-Elander, S., Hansson, P., & Ingvar, M. (1995). Central representation of chronic ongoing neuropathic pain studied by positron emission tomography. *Pain, 63*(2), 225–236.

Iannetti, G. D., Hughes, N. P., Lee, M. C., & Mouraux, A. (2008). Determinants of laser-evoked EEG responses: Pain perception or stimulus saliency? *Journal of Neurophysiology, 100*(2), 815–828.

Jeanmonod, D., & Morel, A. (2009). The central lateral thalamotomy for neuropathic pain. In A. M. Lozano, P. L. Gildenberg, & R. R. Tasker (Eds.), *Textbook of stereotactic and functional neurosurgery* (2nd ed., pp. 2081–2096). Berlin/Heidelberg: Springer.

Jeanmonod, D., Magnin, M., & Morel, A. (1993). Thalamus and neurogenic pain: Physiological, anatomical and clinical data. *Neuroreport, 4*(5), 475–478.

Jeanmonod, D., Magnin, M., & Morel, A. (1994). A thalamic concept of neurogenic pain. In G. Gebhart, D. Hammond, & T. Jensen (Eds.), *Progress in pain research and management* (pp. 767–787). Seattle: IASP Press.

Jeanmonod, D., Magnin, M., & Morel, A. (1996). Low-threshold calcium spike bursts in the human thalamus. Common physiopathology for sensory, motor and limbic positive symptoms. *Brain, 119*(Pt 2), 363–375.

Jeanmonod, D., Magnin, M., Morel, A., & Siegemund, M. (2001a). Surgical control of the human thalamocortical dysrhythmia: I. Central lateral thalamotomy in neurogenic pain. *Thalamus & Related Systems, 1*(1), 71–79.

Jeanmonod, D., Magnin, M., Morel, A., Siegemund, M., Cancro, R., Lanz, M., et al. (2001b). Thalamocortical dysrhythmia II. Clinical and surgical aspects. *Thalamus & Related Systems, 1*, 245–254.

Jones, A. K., Kulkarni, B., & Derbyshire, S. W. (2003a). Pain mechanisms and their disorders. *British Medical Bulletin, 65*, 83–93.

Jones, A. K. P., Kulkarni, B., & Derbyshire, S. W. G. (2003b). Pain mechanisms and their disorders: Imaging in clinical neuroscience. *British Medical Bulletin, 65*(1), 83–93.

Klimesch, W., Schimke, H., Ladurner, G., & Pfurtscheller, G. (1990). Alpha frequency and memory performance. *Journal of Psychophysiology, 4*, 381–390.

Kong, J., White, N. S., Kwong, K. K., Vangel, M. G., Rosman, I. S., Gracely, R. H., et al. (2006). Using fMRI to dissociate sensory encoding from cognitive evaluation of heat pain intensity. *Human Brain Mapping, 27*(9), 715–721.

Kringelbach, M. L., Jenkinson, N., Green, A. L., Owen, S. L., Hansen, P. C., Cornelissen, P. L., et al. (2007). Deep brain stimulation for chronic pain investigated with magnetoencephalography. *Neuroreport, 18*(3), 223–228.

Kupers, R. C., & Gybels, J. M. (1996). *General principles and selection of techniques in the management of pain of benign origin. In: A textbook of stereotactic and functional neurosurgery.* Philadelphia: McGraw-Hill.

Lancaster, J. L., Woldorff, M. G., Parsons, L. M., Liotti, M., Freitas, C. S., Rainey, L., et al. (2000). Automated Talairach Atlas labels for functional brain mapping. *Human Brain Mapping, 10*(3), 120–131.

Landolt, H. P., Retey, J. V., Tonz, K., Gottselig, J. M., Khatami, R., Buckelmuller, I., et al. (2004). Caffeine attenuates waking and sleep electroencephalographic markers of sleep homeostasis in humans. *Neuropsychopharmacology, 29*(10), 1933–1939.

Lee, M. C., & Tracey, I. (2010). Unravelling the mystery of pain, suffering, and relief with brain imaging. *Current Pain and Headache Reports, 14*(2), 124–131.

Legrain, V., Iannetti, G. D., Plaghki, L., & Mouraux, A. (2011). The pain matrix reloaded: A salience detection system for the body. *Progress in Neurobiology, 93*(1), 111–124.

Lenz, F. A., Kwan, H. C., Dostrovsky, J. O., & Tasker, R. R. (1989). Characteristics of the bursting pattern of action potentials that occurs in the thalamus of patients with central pain. *Brain Research, 496*(1–2), 357–360.

Llinás, R., & Jahnsen, H. (1982). Electrophysiology of mammalian thalamic neurones in vitro. *Nature, 297*(5865), 406–408.

Llinas, R., Ribary, U., Contreras, D., & Pedroarena, C. (1998). The neuronal basis for consciousness. *Philosophical Transactions of the Royal Society of London. Series B, Biological Sciences, 353* (1377), 1841–1849.

Llinás, R., Ribary, U., Jeanmonod, D., Kronberg, E., & Mitra, P. P. (1999). Thalamocortical dysrhythmia: A neurological and neuropsychiatric syndrome characterized by magnetoencephalography. *Proceedings of the National Academy of Sciences of the United States of America, 96*(26), 15222–15227.

May, A. (2008). Chronic pain may change the structure of the brain. *Pain, 137*(1), 7–15.

Mazziotta, J., Toga, A., Evans, A., Fox, P., Lancaster, J., Zilles, K., et al. (2001). A probabilistic atlas and reference system for the human brain: International consortium for brain mapping (ICBM). *Philosophical Transactions of the Royal Society of London. Series B, Biological Sciences, 356*(1412), 1293–1322.

Melzack, R., & Casey, K. L. (1968). Sensory, motivation, and central control determinants of pain. In D. R. Kenshalo (Ed.), *The skin senses* (pp. 423–435). Springfield, IL: Thomas.

Mitra, P. P., & Pesaran, B. (1999). Analysis of dynamic brain imaging data. *Biophysical Journal, 76*(2), 691–708.

Moazami-Goudarzi, M., Sarnthein, J., Michels, L., Moukhtieva, R., & Jeanmonod, D. (2008). Enhanced frontal low and high frequency power and synchronization in the resting EEG of parkinsonian patients. *NeuroImage, 41*(3), 985–997.

Moazami-Goudarzi, M., Michels, L., Weisz, N., & Jeanmonod, D. (2010). Temporo-insular enhancement of EEG low and high frequencies in patients with chronic tinnitus. *BMC Neuroscience, 11*(1), 40.

Mobascher, A., Brinkmeyer, J., Warbrick, T., Musso, F., Wittsack, H. J., Saleh, A., et al. (2009). Laser-evoked potential P2 single-trial amplitudes covary with the fMRI BOLD response in the medial pain system and interconnected subcortical structures. *NeuroImage, 45*(3), 917–926.

Moisset, X., & Bouhassira, D. (2007). Brain imaging of neuropathic pain. *NeuroImage, 37*(Suppl 1), S80–S88.

Morel, A., Magnin, M., & Jeanmonod, D. (1997). Multiarchitectonic and stereotactic atlas of the human thalamus. *The Journal of Comparative Neurology, 387*(4), 588–630.

Napflin, M., Wildi, M., & Sarnthein, J. (2007). Test-retest reliability of resting EEG spectra validates a statistical signature of persons. *Clinical Neurophysiology, 118*(11), 2519–2524.

Nichols, T. E., & Holmes, A. P. (2002). Nonparametric permutation tests for functional neuroimaging: A primer with examples. *Human Brain Mapping, 15*(1), 1–25.

Nielen, M. M., Heslenfeld, D. J., Heinen, K., Van Strien, J. W., Witter, M. P., Jonker, C., et al. (2009). Distinct brain systems underlie the processing of valence and arousal of affective pictures. *Brain and Cognition, 71*(3), 387–396.

Nir, R. R., Sinai, A., Raz, E., Sprecher, E., & Yarnitsky, D. (2010). Pain assessment by continuous EEG: association between subjective perception of tonic pain and peak frequency of alpha oscillations during stimulation and at rest. *Brain Research, 1344*, 77–86.

Northoff, G., Richter, A., Gessner, M., Schlagenhauf, F., Fell, J., Baumgart, F., et al. (2000). Functional dissociation between medial and lateral prefrontal cortical spatiotemporal activation in negative and positive emotions: A combined fMRI/MEG study. *Cerebral Cortex, 10*(1), 93–107.

Pascual-Marqui, R. D., Michel, C. M., & Lehmann, D. (1994). Low resolution electromagnetic tomography: A new method for

localizing electrical activity in the brain. *International Journal of Psychophysiology, 18*(1), 49–65.

Percival, D. B., & Walden, A. T. (1993). *Spectral analysis for physical applications*. Cambridge: Cambridge University Press.

Petrovic, P., Carlsson, K., Petersson, K. M., Hansson, P., & Ingvar, M. (2004). Context-dependent deactivation of the amygdala during pain. *Journal of Cognitive Neuroscience, 16*(7), 1289–1301.

Peyron, R., Garcia-Larrea, L., Gregoire, M. C., Convers, P., Richard, A., Lavenne, F., et al. (2000). Parietal and cingulate processes in central pain. A combined positron emission tomography (PET) and functional magnetic resonance imaging (fMRI) study of an unusual case. *Pain, 84*(1), 77–87.

Peyron, R., Laurent, B., & Garcia-Larrea, L. (2000a). Functional imaging of brain responses to pain. A review and meta-analysis. *Neurophysiologie Clinique, 30*(5), 263–288.

Peyron, R., Laurent, B., & Garcia-Larrea, L. (2000b). Functional imaging of brain responses to pain. A review and meta-analysis (2000). *Neurophysiologie Clinique, 30*(5), 263–288.

Pizzagalli, D., Pascual-Marqui, R. D., Nitschke, J. B., Oakes, T. R., Larson, C. L., Abercrombie, H. C., et al. (2001). Anterior cingulate activity as a predictor of degree of treatment response in major depression: Evidence from brain electrical tomography analysis. *The American Journal of Psychiatry, 158*(3), 405–415.

Ploner, M., Gross, J., Timmermann, L., & Schnitzler, A. (2002). Cortical representation of first and second pain sensation in humans. *Proceedings of the National Academy of Sciences of the United States of America, 99*(19), 12444–12448.

Poliakov, I., & Toth, C. (2011). The impact of pain in patients with polyneuropathy. *Eur J Pain*.

Proske, H. J., Jeanmonod, D., & Verschure, P. F. (2011). A computational model of thalamocortical dysrhythmia. *Eur J Neurosci*.

Salomons, T. V., Johnstone, T., Backonja, M. M., Shackman, A. J., & Davidson, R. J. (2007). Individual differences in the effects of perceived controllability on pain perception: critical role of the prefrontal cortex. *Journal of Cognitive Neuroscience, 19*(6), 993–1003.

Sano, K. (1977). Intralaminar Thalamotomy (Thalamolaminotomy) and Postero-Medial Hypothalaomotomy in the treatment of intractable pain. *Progress in Neurological Surgery, 8*, 50–103.

Sarnthein, J., & Jeanmonod, D. (2008). High thalamocortical theta coherence in patients with neurogenic pain. *NeuroImage, 39*(4), 1910–1917.

Sarnthein, J., Stern, J., Aufenberg, C., Rousson, V., & Jeanmonod, D. (2006). Increased EEG power and slowed dominant frequency in patients with neurogenic pain. *Brain, 129*(Pt 1), 55–64.

Schulman, J., Ramirez, R., Zonenshayn, M., Ribary, U., & Llinas, R. (2005). Thalamocortical dysrhythmia syndrome: MEG imaging of neuropathic pain. *Thalamus & Related Systems, 3*(1), 33–39.

Shibasaki, H. (2004). Central mechanisms of pain perception. *Supplements to Clinical Neurophysiology, 57*, 39–49.

Shulman, G., Ramirez, R., Zonenshayn, M., Ribary, U., & Llinas, R. (2005). Thalamocortical dysrhythmia syndrome: MEG imaging of neuropathic pain. *Thalamus & Related Systems, 3*, 33–39.

Spooner, J., Yu, H., Kao, C., Sillay, K., & Konrad, P. (2007). Neuromodulation of the cingulum for neuropathic pain after spinal cord injury. Case report. *Journal of Neurosurgery, 107*(1), 169–172.

Stancak, A., Polacek, H., Vrana, J., & Mlynar, J. (2007). Cortical oscillatory changes during warming and heating in humans. *Neuroscience, 147*(3), 842–852.

Starr, C. J., Sawaki, L., Wittenberg, G. F., Burdette, J. H., Oshiro, Y., Quevedo, A. S., et al. (2009). Roles of the insular cortex in the modulation of pain: insights from brain lesions. *Journal of Neuroscience, 29*(9), 2684–2694.

Steriade, M., Jones, E. G., & McCormick, D. A. (1997). *Thalamus: Organisation and function* (Vol. 1). Oxford: Elsevier.

Stern, J., Jeanmonod, D., & Sarnthein, J. (2006). Persistent EEG overactivation in the cortical pain matrix of neurogenic pain patients. *NeuroImage, 31*(2), 721–731.

Talairach, J., & Tournoux, P. (1988). *Co-planar stereotaxic atlas of the human brain: Three-dimensional proportional system*. Stuttgart: Georg Thieme.

Talbot, J. D., Marrett, S., Evans, A. C., Meyer, E., Bushnell, M. C., & Duncan, G. H. (1991). Multiple representations of pain in human cerebral cortex. *Science, 251*(4999), 1355–1358.

Tracey, I. (2005). Nociceptive processing in the human brain. *Current Opinion in Neurobiology, 15*(4), 478–487.

Tracey, I. (2007). Neuroimaging of pain mechanisms. *Current Opinion in Supportive and Palliative Care, 1*(2), 109–116.

Treede, R. D., Kenshalo, D. R., Gracely, R. H., & Jones, A. K. (1999). The cortical representation of pain. *Pain, 79*(2–3), 105–111.

Treede, R. D., Lorenz, J., & Baumgartner, U. (2003). Clinical usefulness of laser-evoked potentials. *Neurophysiologie Clinique, 33*(6), 303–314.

Wager, T. D., Rilling, J. K., Smith, E. E., Sokolik, A., Casey, K. L., Davidson, R. J., et al. (2004). Placebo-induced changes in FMRI in the anticipation and experience of pain. *Science, 303*(5661), 1162–1167.

Walton, K. D., Dubois, M., & Llinas, R. R. (2010). Abnormal thalamocortical activity in patients with complex regional pain syndrome (CRPS) Type I. *Pain, in press*.

Willis, W. D., Jr. (1985). Pain pathways in the primate. *Progress in Clinical and Biological Research, 176*, 117–133.

Willis, W. D., & Westlund, K. N. (1997). Neuroanatomy of the pain system and of the pathways that modulate pain. *Journal of Clinical Neurophysiology, 14*(1), 2–31.

Willoch, F., Rosen, G., Tolle, T. R., Oye, I., Wester, H. J., Berner, N., et al. (2000). Phantom limb pain in the human brain: unraveling neural circuitries of phantom limb sensations using positron emission tomography. *Annals of Neurology, 48*(6), 842–849.

Wydenkeller, S., Maurizio, S., Dietz, V., & Halder, P. (2009). Neuropathic pain in spinal cord injury: Significance of clinical and electrophysiological measures. *European Journal of Neuroscience, 30*(1), 91–99.